NUREG/CR-1843
ORNL/NUREG/CSD/TM-18
Dist. Category RF

NOZ-FLAW: A FINITE ELEMENT PROGRAM FOR DIRECT EVALUATION OF STRESS INTENSITY FACTORS FOR PRESSURE VESSEL NOZZLE-CORNER FLAWS

S. N. Atluri**
B. R. Bass
J. W. Bryson*
K. Kathiresan**

Sponsor: G. D. Whitman

Manuscript Completed - November 1980
Date Published - March 1981

Prepared for the
Office of Nuclear Regulatory Research
U. S. Nuclear Regulatory Commission
Washington, DC 20555
Under Interagency Agreements DOE 40-551-75 and 40-552-75

NRC FIN No. B0119

*Engineering Technology Division, Oak Ridge National Laboratory, Oak Ridge, TN 37830

**Georgia Institute of Technology, Atlanta, GA 30332

COMPUTER SCIENCES DIVISION
at
Oak Ridge Gaseous Diffusion Plant
Post Office Box P
Oak Ridge, Tennessee 37830

Union Carbide Corporation, Nuclear Division
operating the
Oak Ridge Gaseous Diffusion Plant . Oak Ridge National Laboratory
Oak Ridge Y-12 Plant . Paducah Gaseous Diffusion Plant
under Contract No. W-7405-eng-26
for the
Department of Energy

8105120060

TABLE OF CONTENTS

LIST OF FIGURES

LIST OF FIGURES (cont'd)

FOREWORD

The work reported here was performed at the Oak Ridge National Laboratory and at the Georgia Institute of Technology under UCC-ND Subcontract No. 7565. This work is sponsored by the U.S. Nuclear Regulatory Commission's (NRC) Heavy-Section Steel Technology (HSST) Program which is directed at ORNL by G. D. Whitman. The manager for the NRC is M. Vagins.

Prior HSST technical reports are listed below:

1. S. Yukawa, Evaluation of Periodic Proof Testing and Warm Prestressing Procedures for Nuclear Reactor Vessels, HSSTP-TR-1, General Electric Company, Schenectady, NY (July 1, 1969).

2. L. W. Loechel, The Effect of Testing Variables on the Transition Temperature in Steel, MCR-69-189, Martin Marietta Corporation, Denver, CO (November 20, 1969).

3. P. N. Randall, Gross Strain Measure of Fracture Toughness of Steels, HSSTP-TR-3, TRW Systems Group, Redondo Beach, CA (November 1, 1969).

4. C. Visser, S.E. Gabrielse, and W. VanBuren, A Two-Dimensional Elastic-Plastic Analysis of Fracture Test Specimens, WCAP-7368, Westinghouse Electric Corporation, PWR Systems Division, Pittsburgh, PA (October 1969).

5. T. R. Mager and F. O. Thomas, Evaluation by Linear Elastic Fracture Mechanics of Radiation Damage to Pressure Vessel Steels, WCAP-7328 (Rev.), Westinghouse Electric Corporation, PWR Systems Division, Pittsburgh, PA (October 1969).

6. W. O. Shabbits, W. H. Pryle, and E. T. Wessel, Heavy Section Fracture Toughness Properties of A533 Grade B Class 1 Steel Plate and Submerged Arc Weldment, WCAP-7414, Westinghouse Electric Corporation, PWR Systems Division, Pittsburgh, PA (December 1969).

7. F. J. Loss, Dynamic Tear Test Investigations of the Fracture Toughness of Thick-Section Steel, NRL-7056. Naval Research Laboratory, Washington, DC (May 14, 1970).

8. P. B. Crosley and E. J. Ripling, Crack Arrest Fracture Toughness of A533 Grade B Class 1 Pressure Vessel Steel, HSSTP-TR-8, Materials Research Laboratory, Inc., Glenwood, IL (March 1970).

9. T. R. Mager, Post-Irradiation Testing of 2T Compact Tension Specimens, WCAP-7561, Westinghouse Electric Corporation, PWR Systems Division, Pittsburgh, PA (August 1970).

10. T. R. Mager, Fracture Toughness Characterization Study of A533, Grade B,Class 1 Steel, WCAP-7578, Westinghouse Electric Corporation, PWR Systems Division, Pittsburgh, PA (October 1970).

11. T. R. Mager, Notch Preparation in Compact Tension Specimens, WCAP-7579, Westinghouse Electric Corporation, PWR Systems Division, Pittsburgh, PA (November 1970).

12. N. Levy and P. V. Marcal, Three Dimensional Elastic-Plastic Stress and Strain Analysis for Fracture Mechanics, Phase I: Simple Flawed Specimens, HSSTP-12, Brown University, Providence, RI (December 1970).

13. W. O. Shabbits, Dynamic Fracture Toughness Properties of Heavy Section A533 Grade B Class 1 Steel Plate, WCAP-7623, Westinghouse Electric Corporation, PWR Systems Division, Pittsburgh, PA (December 1970).

14. P. N. Randall, Gross Strain Crack Tolerance of A533-B Steel, HSSTP-TR-14, TRW Systems Group, Redondo Beach, CA (May 1, 1971).

15. H. T. Corten and R. H. Sailors, Relationship Between Material Fracture Toughness Using Fracture Mechanics and Transition Temperature Tests, T&AM Report 346, University of Illinois, Urbana, IL (August 1, 1971).

16. T. R. Mager and V. J. McLaughlin, The Effect of an Environment of High Temperature Primary Grade Nuclear Reactor Water on the Fatigue Crack Growth Characteristics of A533 Grade B Class 1 Plate and Weldment Material, WCAP-7776, Westinghouse Electric Corporation, PWR Systems Division, Pittsburgh, PA (October 1971).

17. N. Levy and P. V. Marcal, Three-Dimensional Elastic-Plastic Stress and Strain Analysis for Fracture Mechanics, Phase II: Improved Modeling HSSTP-TR-17, Brown University, Providence, RI (November 1971).

18. S. C. Grigory, Tests of 6-Inch-Thick Flawed Tensile Specimens, First Technical Summary Report, Longitudinal Specimens Numbers 1 through 7, HSSTP-TR-18, Southwest Research Institute, San Antonio, TX (June 1972).

19. P. N. Randall, Effects of Strain Gradients on the Gross Strain Crack Tolerance of A533-B Steel, HSSTP-TR-19, TRW Systems Group, Redondo Beach, CA (June 15, 1972).

20. S. C. Grigory, Tests of 6-Inch-Thick Flawed Tensile Specimens, Second Technical Summary Report, Transverse Specimens Numbers 8 through 10, Welded Specimens Numbers 11 through 13, HSSTP-TR-20, Southwest Research Institute, San Antonio, TX (June 1972).

21. L. A. James and J. A. Williams, Heavy Section Steel Technology Program Technical Report No. 21, The Effect of Temperature and Neutron Irradiation Upon the Fatigue-Crack Propagation Behavior of ASTM A533 Grade B, Class 1 Steel, HEDL-TME 71-132, Hanford Engineering Development Laboratory, Richland, WA (September 1972).

22. S. C. Grigory, Tests of 6-Inch-Thick Flawed Tensile Specimens, Third Technical Summary Report, Longitudinal Specimens Numbers 14 through 16, Unflawed Specimens Number 17, HSSTP-TR-22, Southwest Research Institute, San Antonio, TX (October 1972).

23. S. C. Grigory, Tests of 6-Inch-Thick Tensile Specimens, Fourth Technical Summary Report, Tests of 1-Inch-Thick Flawed Tensile Specimens for Size Effect Evaluation, HSSTP-TR-23, Southwest Research Institute, San Antonio, TX (June 1973).

24. S. P. Ying and S. C. Grigory, Test of 6-Inch-Thick Tensile Specimens, Fifth Technical Summary Report, Acoustic Emisson Monitoring of One-Inch and Six-Inch-Thick Tensile Specimens, HSSTP-TR-24, Southwest Research Institute, San Antonio, TX (November 1972).

25. R. W. Derby, J. G. Merkle, G. C. Robinson, G. D. Whitman and F. J. Witt, Test of 6-Inch-Thick Pressure Vessels. Series 1: Intermediate Test Vessels V-1 and V-2, ORNL-4895, Oak Ridge National Laboratory, Oak Ridge TN (February 1974).

26. W. J. Stelzman and R. G. Berggren, Radiation Strengthening and Embrittlement in Heavy Section Steel Plates and Welds, ORNL-4871, Oak Ridge National Laboratory, Oak Ridge, TN (June 1973).

27. P. B. Crosley and E. J. Ripling, Crack Arrest in an Increasing K-Field, HSSTP-27, Materials Research Laboratory, Inc., Glenwood, IL (January 1973).

28. P. V. Marcal, P. M. Stuart, and R. S. Bettes, Elastic Plastic Behavior of a Longitudinal and Semi-Elliptic Crack in a Thick Pressure Vessel, HSSTP-TR-28, Brown University, Providence, RI (June 1973).

29. W. J. Stelzman, Characterization of HSST Plate 02 (in preparation).

30. D. A. Canonico, Characterization of Heavy Section Weldments in Pressure Vessel Steels (in preparation).

31. J. A. Williams, The Irradiation and Temperature Dependence of Tensile and Fracture Properties of ASTM A533, Grade B, Class 1 Steel Plate and Weldment, HEDL-TME 73-75, Hanford Engineering Development Laboratory, Richland, WA (August 1973).

32. J. M. Steichen and J. A. Williams, High Strain Rate Tensile Properties of Irradiated ASTM A533 Grade B Class 1 Pressure Vessel Steel, Hanford Engineering Development Laboratory, Richland, WA (July 1973).

33. P. C. Riccardella and J. L. Swedlow, A Combined Analytical-Experimental Fracture Study of the Two Leading Theories of Elastic-Plastic Fracture (J-Integral and Equivalent Energy), WCAP-8224, Westinghouse Electric Corporation, Pittsburgh, PA (October 1973).

34. R. J. Podlasek and R. J. Eiber, Final Report on Investigation of Mode III Crack Extension in Reactor Piping, Battelle Columbus Laboratories, Columbus, OH (Dec. 14, 1973).

35. T. R. Mager, J. D. Landes, D. M. Moon and V. J. McLaughlin, Interim Report on the Effect of Low Frequencies on the Fatigue Crack Growth Characteristics of A533 Grade B Class 1 Plate in an Environment of High-Temperature Primary Grade Nuclear Peactor Water, WCAP-8526, Westinghouse Electric Corporation, Pittsburgh, PA (December 1973).

36. J. A. Williams, The Irradiated Fracture Toughness of ASTM A533, Grade B, Class 1 Steel Measured with a Four-Inch-Thick Compact Tension Specimen, HEDL-TME 75-10, Hanford Engineering Development Laboratory, Richland, WA (January 1975).

37. R. H. Bryan, J. G. Merkle, M. N. Raftenberg, G. C. Robinson and J. E. Smith, Test of 6-Inch-Thick Pressure Vessels. Series 2: Intermediate Test Vessels, V-3, V-4, and V-6, ORNL-5059, Oak Ridge National Laboratory, Oak Ridge, TN (November 1975).

38. T. R. Mager, S. E. Yanichko, and L. R. Singer, Fracture Toughness Characterization of HSST Intermediate Pressure Vessel Material, WCAP-8456, Westinghouse Electric Corporation, Pittsburgh, PA (December 1974).

39. J. G. Merkle, G. D. Whitman, and R. H. Bryan, An Evaluation of the HSST Program Intermediate Pressure Vessel Tests in Terms of Light-Water-Reactor Pressure Vessel Safety, ORNL/TM-5090, Oak Ridge National Laboratory, Oak Ridge, TN (November 1975).

40. J. G. Merkle, G. C. Robinson, P. P. Holz, J. E. Smith and R. H. Bryan, Test of 6-Inch-Thick Pressure Vessels. Series 3: Intermediate Test Vessel V-7, ORNL/NUREG-1, Oak Ridge National Laboratory, Oak Ridge, TN (August 1976).

41. J. A. Davidson, L. J. Ceschini, R. P. Shogan, and G. V. Rao, The Irradiated Dynamic Fracture Toughness of ASTM A533, Grade B, Class 1 Steel Plate and Submerged Arc Weldment, WCAP-875, Westinghouse Electric Corporation, Pittsburgh, PA (October 1976).

42. R. D. Cheverton, Pressure Vessel Fracture Studies Pertaining to a PWR LOCA-ECC Thermal Shock: Experiments TSE-1 and TSE-2, ORNL/NUREG/TM-31, Oak Ridge National Laboratory, Oak Ridge, TN (September 1976).

43. J. G. Merkle, G. C. Robinson, P. P. Holz and J. E. Smith, Test of 6-Inch-Thick Pressure Vessels. Series 4: Intermediate Test Vessels V-5 and V-9 with Inside Nozzle Corner Cracks, ORNL/NUREG-7, Oak Ridge National Laboratory, Oak Ridge, TN (August 1977).

44. J. A. Williams, The Ductile Fracture Toughness of Heavy Section Steel Plate, Hanford Engineering Development Laboratory, Richland, WA, NUREG/CR-0859 (September 1979).

45. R. H. Bryan, T. M. Cate, P. P. Holz, T. A. King, J. G. Merkle, G. C. Robinson, G. C. Smith, J. E. Smith and G. D. Whitman, Test of 6-Inch-Thick Pressure Vessels. Series 3: Intermediate Test Vessel V-7A Under Sustained Loading, ORNL/NUREG-9, Oak Ridge National Laboratory, Oak Ridge, TN (February 1978).

46. R. D. Cheverton and S. E. Bolt, Pressure Vessel Fracture Studies Pertaining to a PWR LOCA-ECC Thermal Shock: Experiments TSE-3 and TSE-4 and Update of TSE-1 and TSE-2 Analysis, ORNL/NUREG-22, Oak Ridge National Laboratory, Oak Ridge, TN (December 1977).

47. D. A. Canonico, Significance of Reheat Cracks to the Integrity of Pressure Vessels for Light-Water Reactors, ORNL/NUREG-15, Oak Ridge National Laboratory, Oak Ridge, TN (July 1977).

48. G. C. Smith and P. P. Holz, Repair Weld Induced Residual Stresses in Thick-Walled Steel Pressure Vessels, NUREG/CR-0093 (ORNL/NUREG/TM-153), Oak Ridge National Laboratory, Oak Ridge, TN (June 1978).

49. P. P. Holz and S. W. Wismer, Half-Bead (Temper) Repair Welding for HSST Vessels, NUREG/CR-0113 (ORNL/NUREG/TM-177), Oak Ridge National Laboratory, Oak Ridge, TN (June 1978).

50. G. C. Smith, P. P. Holz and W. J. Stelzman, Crack Extension and Arrest Tests of Axially Flawed Steel Model Pressure Vessels, NUREG/CR-0126 (ORNL/NUREG/TM-196), Oak Ridge National Laboratory, Oak Ridge, TN (October 1978).

51. R. H. Bryan, P. P. Holz, J. G. Merkle, G. C. Smith, J. E. Smith and W. J. Stelzman, Test of 6-Inch-Thick Pressure Vessels. Series 3: Intermediate Test Vessel V-7B, NUREG/CR-0309 (ORNL/NUREG-38), Oak Ridge National Laboratory, Oak Ridge, TN (October 1978).

52. R. D. Cheverton, S. K. Iskander and S. E. Bolt, Applicability of LEFM to the Analysis of PWR Vessels Under LOCA-ECC Thermal Shock Conditions, NUREG/CR-0107 (ORNL/NUREG-40), Oak Ridge National Laboratory, Oak Ridge, TN (October 1978).

53. R. H. Bryan, D. A. Canonico, P. P. Holz, S. K. Iskander, J. G. Merkle, J. E. Smith and W. J. Stelzman, Test of 6-Inch-Thick Pressure Vessels. Series 3: Intermediate Test Vessel V-8, NUREG/CR-0675 (ORNL/NUREG-58), Oak Ridge National Laboratory, Oak Ridge, TN (December 1979).

54. R. D. Cheverton, Application of Static and Dynamic Crack Arrest Theory to TSE-4, NUREG/CR-0767 (ORNL/NUREG-57), Oak Ridge National Laboratory, Oak Ridge, TN (June 1979).

55. J. A. Williams, Tensile Properties of Irradiated and Unirradiated Welds of A533 Steel Plate and A508 Forgings, Hanford Engineering Development Laboratory, Richland, WA, NUREG/CR-1158, ORNL/Sub-79-50917/2 (July 1979).

56. K. W. Carlson and J. A. Williams, The Effect of Crack Length and Side Groove on the Ductile Fracture Toughness Properties of ASTM A533 Steel, Hanford Engineering Development Laboratory, Richland, WA, NUREG/CR-1171, ORNL/Sub-79-50917/3 (October 1979).

57. P. P. Holz, Flaw Preparations for HSST Program Vessel Fracture Mechanics Testing, Mechanical-Cyclic Pumping and Electron-Beam Weld-Hydrogen Charge Cracking Schemes, NUREG/CR-1274 (ORNL/NUREG/TM-369), Oak Ridge National Laboratory, Oak Ridge, TN (May 1980).

58. S. K. Iskander, Two Finite Element Techniques for Computing Mode I Stress Intensity Factors in Two- or Three-Dimensional Problems, NUREG/CR-1499 (ORNL/NUREG/CSD/TM-14), Computer Sciences Division, Union Carbide Corporation, Nuclear Division (in preparation).

NOZ-FLAW: A FINITE ELEMENT PROGRAM FOR DIRECT EVALUATION OF STRESS INTENSITY FACTORS FOR PRESSURE VESSEL NOZZLE-CORNER FLAWS

S. N. Atluri
B. R. Bass
J. W. Bryson
K. Kathiresan

ABSTRACT

This report describes a linear elastic finite element computer program (NOZ-FLAW) which is used for the direct evaluation of mixed-mode stress intensity factors (K_I, K_{II}, K_{III}) along user-defined crack flaws at pressure-vessel nozzle corners. Special three-dimensional crack front elements are used to model the immediate vicinity of the flaw. These crack front elements have the proper square root and inverse square root variations for displacements and stresses, respectively. Regular isoparametric elements are used away from the flaw front. Inter-element displacement compatibility between singular and regular elements is satisified by assuming an independent boundary displacement field and using a Lagrange multiplier technique to enforce the compatibility constraint. The stress intensity factors at various points on the crack front are solved for directly along with the unknown nodal displacements. The program provides for automatic generation of a finite element model incorporating either a mathematical or user-defined crack flaw. Generation and analysis of the model are performed with program input consisting of 8 to 12 cards. Applications of the program to several crack flaws in an intermediate test vessel are described.

1. INTRODUCTION

A primary concern in the fracture safety analysis of a nuclear pressure vessel is the nozzle corner flaw located in the longitudinal plane, i.e., the plane containing both the nozzle and vessel axes (see Figure 1). Under cyclic pressure loading, the high hoop stresses at the inside nozzle corner may promote both initiation and propagation of such flaws. Certain cyclic pressure experiments [1] have shown that fatigue cracks form first at this location. In addition, such cracks have occurred from thermal fatigue in boiling water reactor feedwater nozzles [2]. These flaws may lead to fast fracture at low temperatures if they grow by fatigue to a critical size. Thus, development of accurate fracture analysis methods applicable to such flaws is essential to assessing the structural integrity of reactor vessels.

In applications of linear elastic fracture mechanics (LEFM) to three-dimensional structures, the intensity of the elevated stress field near a crack flaw is characterized by mixed-mode stress intensity factors K_I, K_{II} and K_{III} that depend upon geometry and applied loading (see, for example, [3]). These factors have been accepted as the appropriate parameters governing fatigue crack propagation and failure by brittle fracture. For nozzle corner flaws, the evaluation of these K-factors is complicated by the geometry of the nozzle-vessel junction containing the flaw , as well as by the complex state of stress present for loadings of practical interest. A further complication arises from the stress intensity factors being undefined at the nozzle and vessel free surfaces. An early attempt to estimate K-factors for a nozzle corner crack was made by Yukawa [4]. He combined the known solutions for a through crack emanating from a circular hole in a flat plate under uniaxial and equibiaxial tension [5] with a crack-shape reduction factor. This factor was based on the ratio of the stress intensity factor for a corner crack [6] to that for a through edge crack in a rectangular bar under uniform tension. More recently, various finite element methods have been employed [7-12]. Alternative numerical methods which generally require a solution for the hoop stresses in the crack area of the uncracked geometry have also been developed [13-16]. Stress intensity factors for nozzle corner flaws have been experimentally determined from burst tests on epoxy models [17] and from frozen-stress photoelastic techniques [18,19].

ORNL-DWG 80-16639

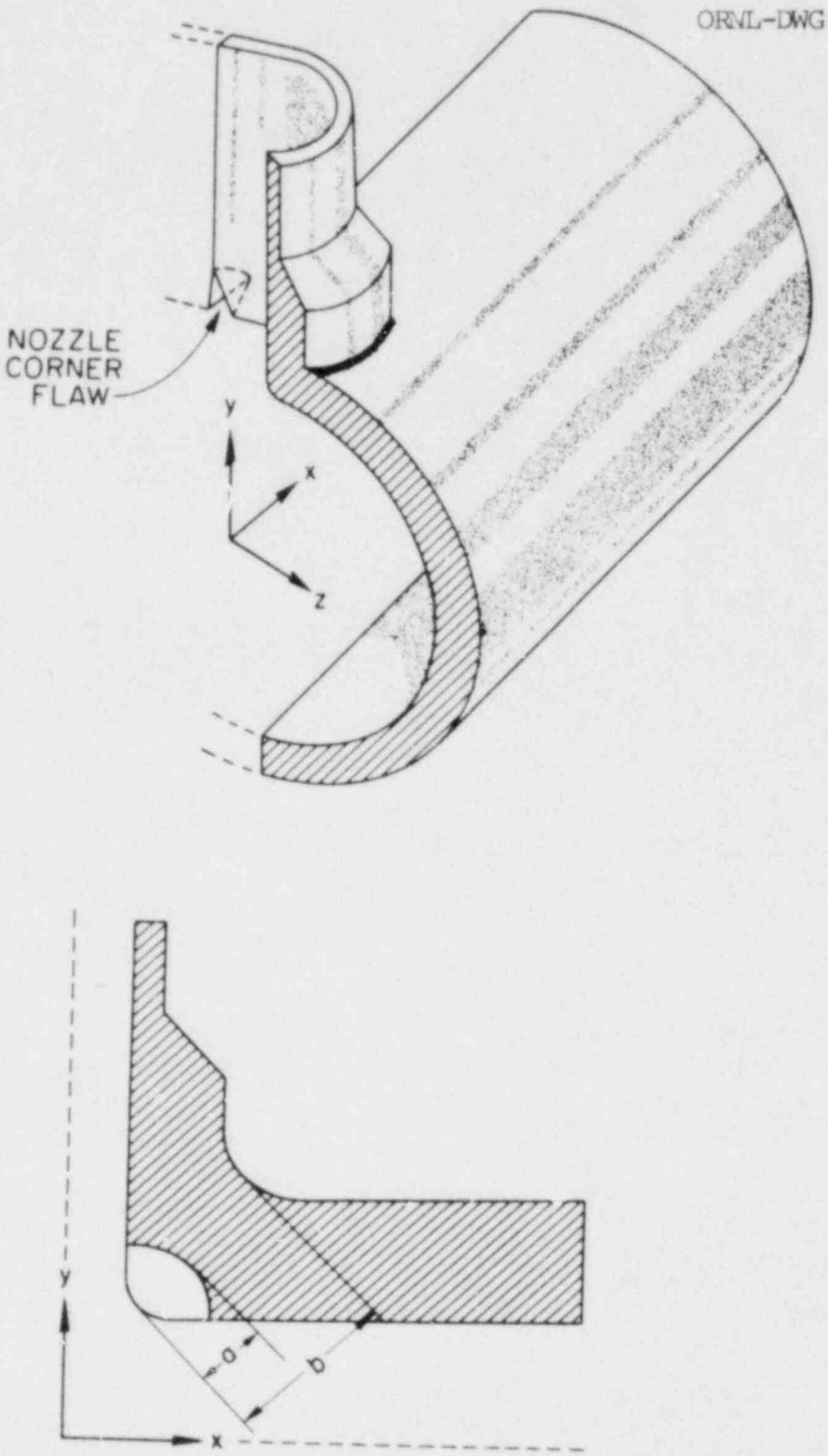

Figure 1. Nozzle corner flaw in longitudinal plane

A critical evaluation of these results indicates that calculation of reliable stress intensity factors for nozzle corner flaws is still very much an open issue. For example, investigators have reported significantly different variations of the mode I factor, K_I, along the crack front for similar geometries and applied loads. Most of the numerical procedures compute a K_I variation that has a relative maximum near the free surface and a relative minimum near the midpoint of the crack front (see, for example, [10-15]). In contrast, the photoelastic results of References 18, 19 demonstrate an opposite trend. Furthermore, most of the numerical techniques to date introduce simplifications or approximations necessary to make the nozzle corner flaw problem mathematically tractable. Modeling the crack flaw as a quarter circle or quarter ellipse is a typical device, whereas certain experimental evidence [18,19] indicates that this may be an oversimplification.

The need for improved fracture analysis capability in reactor safety research has prompted the Nuclear Regulatory Commission (NRC) to sponsor development of a linear elastic finite element program designed to calculate mixed-mode K-factors for nozzle corner flaws. Funding of this work is through the Heavy Section Steel Technology (HSST) program at the Oak Ridge National Laboratory (ORNL). The computer program NOZ-FLAW described herein is a product of this effort. Development of program NOZ-FLAW was initiated under a subcontract to Professor S. N. Atluri at the Georgia Institute of Technology, with Dr. K. Kathiresan responsible for program design. The core of NOZ-FLAW was formed, prior to ORNL sponsorship, by installing a special hybrid-displacement crack-tip element proposed by Atluri and Kathiresan [20,21] in the three-dimensional finite element program TEXGAP3D [22]. This program was then interfaced with the automatic mesh generator module AUTO, also developed under the subcontract, to complete the NOZ-FLAW package. Module AUTO was designed to produce a complete finite element model of a reinforced nozzle-cylinder connection containing a corner crack flaw using relatively few input cards. However, the subcontract with Professor Atluri expired before AUTO could be made operational according to the original ORNL specifications. Consequently, the NOZ-FLAW package was transmitted to ORNL with the mesh generation feature unfinished.

Technical staff in Computing Applications Engineering Department (CAD) and the HSST program at ORNL assumed responsibility for making NOZ-FLAW operational on the Oak Ridge computers. First, an IBM-compatible source program was developed from Dr. Kathiresan's CDC version, followed by extensive modifications and additions to the AUTO module to activate the automatic mesh generator option. Included in this effort were some limited graphics developments for visual display of the generated finite element models. The completed Oak Ridge version of NOZ-FLAW was then used to analyze several nozzle corner flaws for comparison with other relevant experimental and numerical results, as described in Section 3 of this report.

Program NOZ-FLAW has the following unique features: (1) the capability to model user-defined flaw shapes as well as the mathematical shapes which have been analyzed and reported in the literature; (2) the use of special crack tip elements along the crack front (see Figure 2) which have the proper square root and inverse square root variations in displacements and stresses, respectively; (3) the direct calculation of K-factors, as opposed to previously reported finite element techniques which employ displacement-stress extrapolation schemes or the calculation of strain energy release rates to determine K-values. Other features of the program include automatic mesh generation for a nozzle corner flaw located in the longitudinal plane and the use of regular twenty-node isoparametric elements away from the crack tip.

ORNL-DWG 79 7635

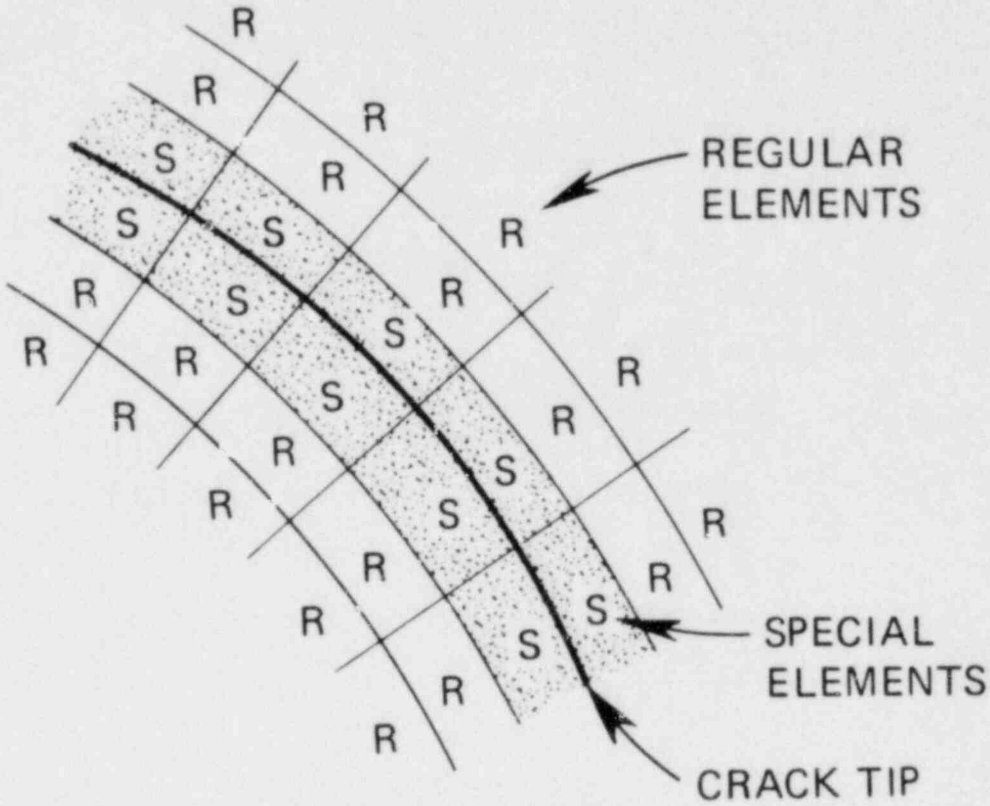

Figure 2. Special crack tip elements along crack front

2. THE NOZ-FLAW COMPUTER PROGRAM

2.1 Capabilities and Limitations

NOZ-FLAW is a linear elastic finite element program which is used for the calculation of mixed-mode stress intensity factors along user-defined crack flaws at pressure-vessel nozzle corners. The crack flaw is assumed to lie in the longitudinal plane (see Figure 1). Special crack tip elements (hybrid-displacement) are used along the crack front and the K-factors are computed directly for each of these special elements.

NOZ-FLAW requires as few as eight cards of input to automatically generate a finite element mesh and perform an analysis. However, the convenience of having very limited user input introduces the following restrictions and limitations in the current version of the program:

(1) The material is linearly elastic, i.e., the plastic zone near the crack tip is ignored;

(2) The crack flaw is positioned in the longitudinal plane; also, certain restrictions on flaw dimensions are discussed in Section 2.3;

(3) A mesh for one-eighth of the configuration is automatically generated and boundary conditions are imposed to model the symmetric configuration shown in Figure 3. Thus, when one uses the present version of NOZ-FLAW to analyze a single nozzle with a single flaw, one assumes that the effects of a second nozzle underneath the vessel as well as the three additional flaws remote from the flaw of interest can be ignored. It is recommended that the present program be used only for relatively small nozzle-to-cylinder diameter ratios.

(4) The loading is due to internal pressure only, with or without crack face pressure;

(5) The nozzle-cylinder junction has ASME code 'standard' reinforcement only;

(6) The junction consists of a single material;

(7) The K-values are constant over an element; therefore, several crack tip elements must be used along the crack front.

ORNL-DWG 80-16648

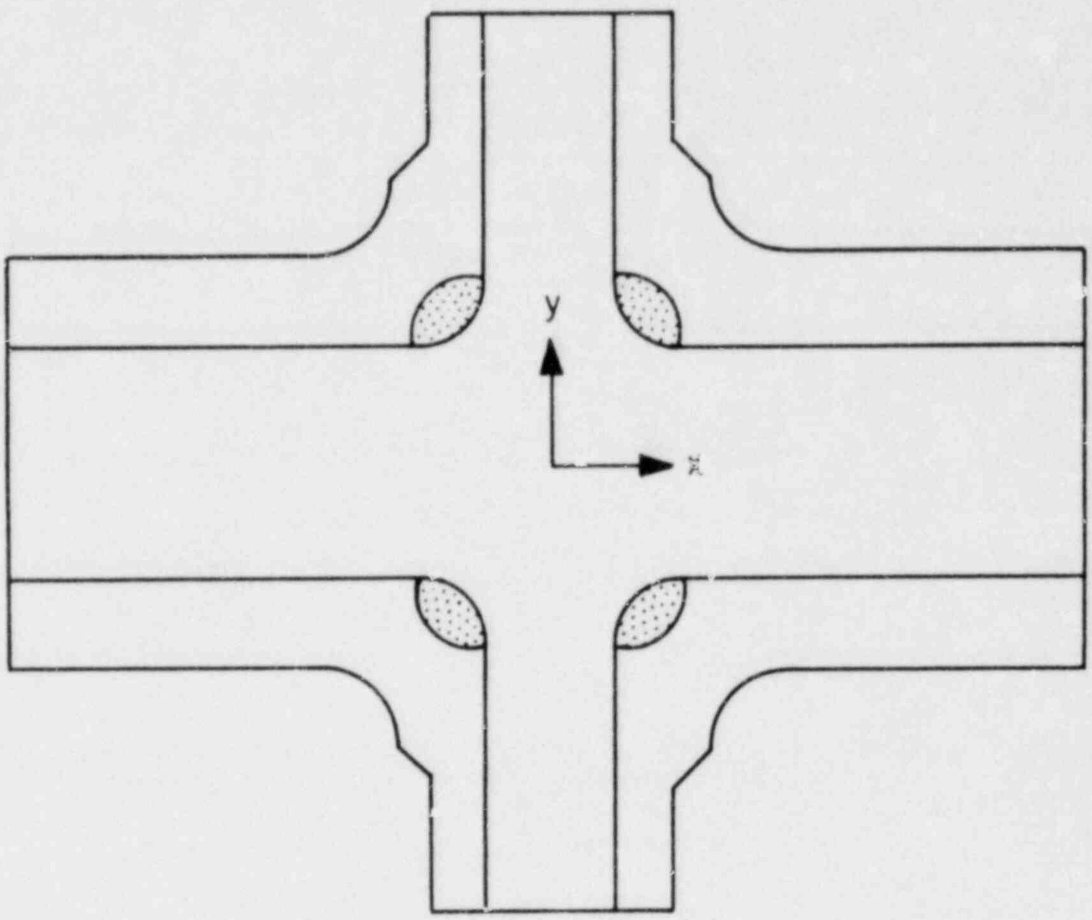

Figure 3. Nozzle corner flaw configuration with threefold symmetry

In addition, the strategy employed in the mesh generator requires that the user define an appropriate mesh in the longitudinal plane which is rotated and distorted to a compatible shape at various intervals around the nozzle. Hence, the mesh refinement at the transverse (y-z) plane is much finer than usually required for an analysis. The mesh generator employs twenty-node brick elements for both regular and singular elements (except at the top of the reinforcement, where prisms are used), producing a model that typically consists of several thousand equations. Substantial computer resources are required by NOZ-FLAW to analyze such a problem, as described in Appendix B.

There are no inherent reasons why restrictions (2) through (6) above could not be relaxed in future versions of the program, as they merely relate to geometry or boundary condition changes. For example, locating the flaw in the transverse plane or other planes would be relatively straightforward since the necessary mesh refinement already exists in these planes. Only the boundary conditions would need to be modified. With some additional effort, other mechanical or even thermal loadings could be considered. Relaxing certain of the above restrictions, however, would certainly increase both the complexity and cost of the analysis.

Printed output from NOZ-FLAW consists of an echo of the input data, element connectivities, nodal global coordinates, imposed boundary conditions, displacements, stresses, and strains throughout the structure and K-values for each of the special crack tip elements along the crack flaw front.

2.2 The Hybrid-Displacement Finite Element Procedure

The special crack tip elements used in NOZ-FLAW were developed using a hybrid-displacement finite element procedure. This procedure has been developed and extensively applied to three-dimensional linear elastic fracture problems by Atluri, Kathiresan, et al. (References 20,21,23-25), and the details of the procedure will not be repeated here. Briefly, the hybrid-displacement finite element method is based on the stationary condition of a modified total potential energy principle. The arbitrary element interior displacements, inter-element boundary displacements, and element boundary tractions (Lagrange multipliers) are the three field variables. Three-dimensional asymptotic solutions for displacements and stresses are embedded in the special crack tip elements. Compatibility between the special crack tip elements and the regular isoparametric elements is enforced through the variational principle, assuring the convergence of the finite element procedure.

Application of the stationary condition yields a set of algebraic equations governing the global nodal displacements $\underline{u}$, and the mode I, II, and III stress intensity factors $\underline{K}$ at various points along the crack front:

$$S_1 \underline{u} + S_2 \underline{K} = \underline{Q}_1$$

$$S_2 \underline{u} + S_3 \underline{K} = \underline{Q}_2 \quad .$$

Here, S_1, S_2, S_3 are the corresponding global stiffness matrices, and $\underline{Q}_1$, $\underline{Q}_2$ are the corresponding global nodal forces. Thus, the stress intensity factors are calculated directly from the governing equations, along with the nodal displacements.

2.3 AUTOmatic Mesh Generation

The automatic mesh generation module AUTO in NOZ-FLAW is designed to generate a three-dimensional finite element model of an isolated nozzle-cylinder connection containing a corner crack flaw, subject to the restrictions outlined below. Isoparametric twenty-node brick type and sixteen-node prism type elements are used throughout the model. As few as eight input cards are required by the program to completely define the finite element model, including the nodal point coordinates, element connectivities, and imposed boundary conditions. A complete description of the required card input is given in the user instructions, Appendix A.

The following assumptions are made in generating the three-dimensional finite element model of the nozzle-cylinder junction with corner flaw.

(1) The nozzle-cylinder junction is fully reinforced as illustrated in Figure 4 (also, Figure NB-3338.2-2 (a) of the ASME Boiler and Pressure Vessel Code).

(2) The nozzle is radially attached to the cylindrical vessel.

(3) The model has inner and outer surface transitions (r_1 and r_2 of Figure 4) between the nozzle and vessel. These transitions are circular arcs arcs and connect tangentially with the cylindrical nozzle and cylindrical vessel.

(4) The part-through corner flaw is positioned in the x-y plane (also identified as the longitudinal plane) of Figure 1.

ORNL-DWG 80-16645

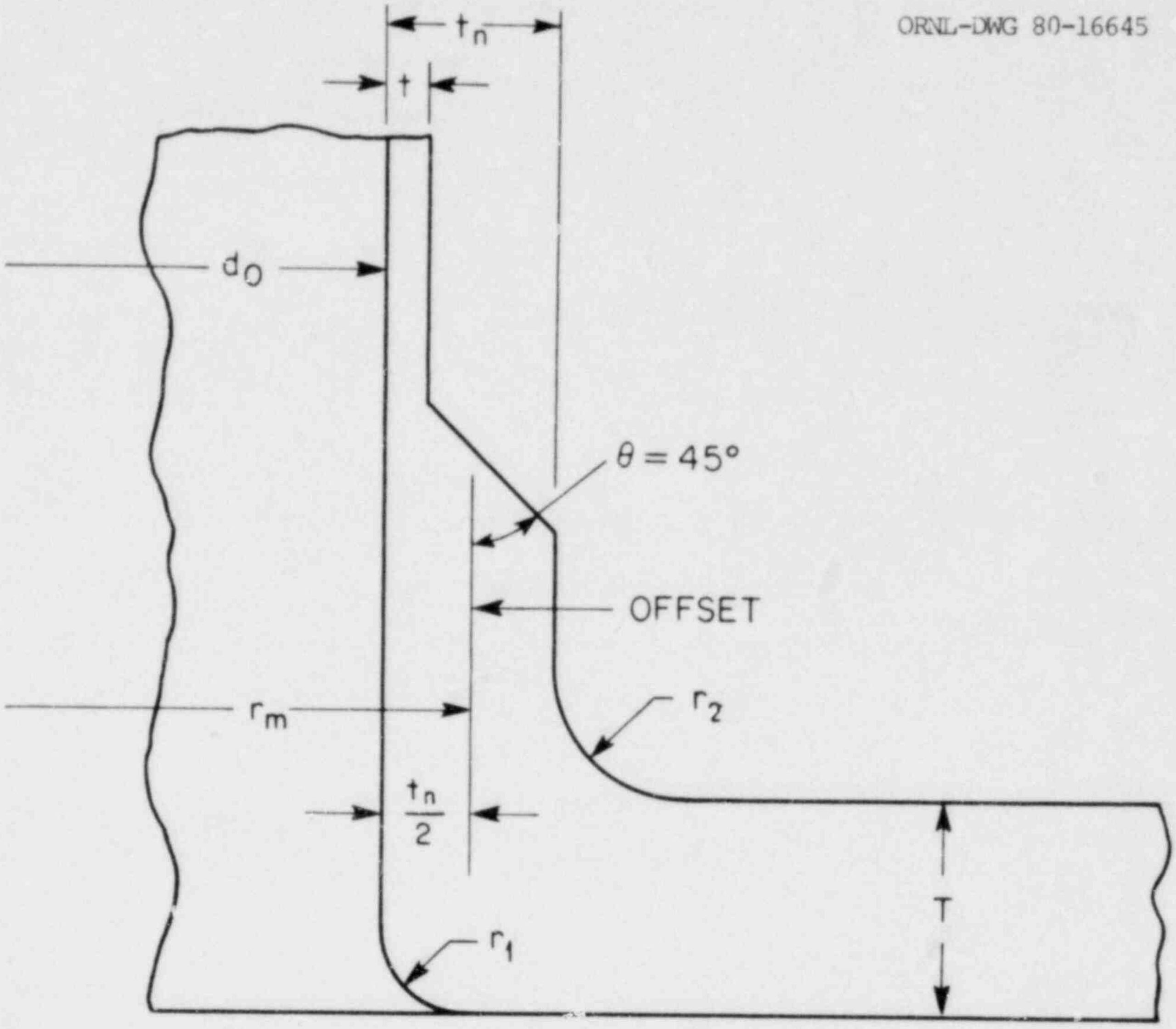

Figure 4. ASME code standard reinforcement design

(5) The geometric parameters of the nozzle corner flaw model, defined on cards D-F of the user instructions, satisfy the following inequality:[1]

$$(PNR + CRA + 2.* SIZE) < 0.95 * PVR$$

(If the option EXPR is chosen, then CRA is replaced by X(1) of card F.)

(6) The nozzle-vessel configuration has three planes of symmetry as shown in Figure 3. This assumption is discussed further in the next section.

In constructing the finite element model, AUTO divides the generation of the node point coordinates into two distinct steps. The first step consists of defining the coordinates of nodes positioned in the x-y or longitudinal plane of the model. This is accomplished in subroutine NCNSTR by positioning nodes for the special crack tip elements along arcs that parallel the mathematically defined or experimentally measured crack front (region I of Figure 5). The location of the crack front and number of divisions in this region are controlled by input parameters on cards D-F. The definition of the longitudinal cross section is completed by a rectangular discretization of the cylindrical vessel (region II) and the nozzle reinforcement (region III).

In the second phase of the node point generation scheme, subroutine NCNST1 'rotates' the nodes in the longitudinal plane about the nozzle and/or vessel axes, defining the nodal coordinates in appropriately positioned meridional planes. The details of this scheme, including the relevant equations, are analogous to those described in Chapter 2 of Reference 26, and will not be given here. The number of meridional planes is controlled by the parameter NZ on Card E. The node point generation process terminates with the specification of nodal coordinates on the transverse plane (y-z plane, Figure 1).

With generation of the node point coordinates thus completed, program AUTO calls subroutine ELEMNT to define element types and nodal connectivities. In ELEMNT, the element types (brick, prism, or crack tip) are identified and numbered in sequence from the longitudinal to the transverse plane. Figures 6 through 8 illustrate the element numbering system generated by NOZ-FLAW for an Intermediate Test Vessel (ITV) model with a quarter-circular nozzle corner flaw. The nodal connectivity and face numbering scheme for the twenty-node isoparametric element are shown in Figure 9. The orientation of the

---

[1] This inequality is required by the algorithm used in the node point coordinate generating routine NCNST1 in the AUTO module.

ORNL-DWG 80-16647

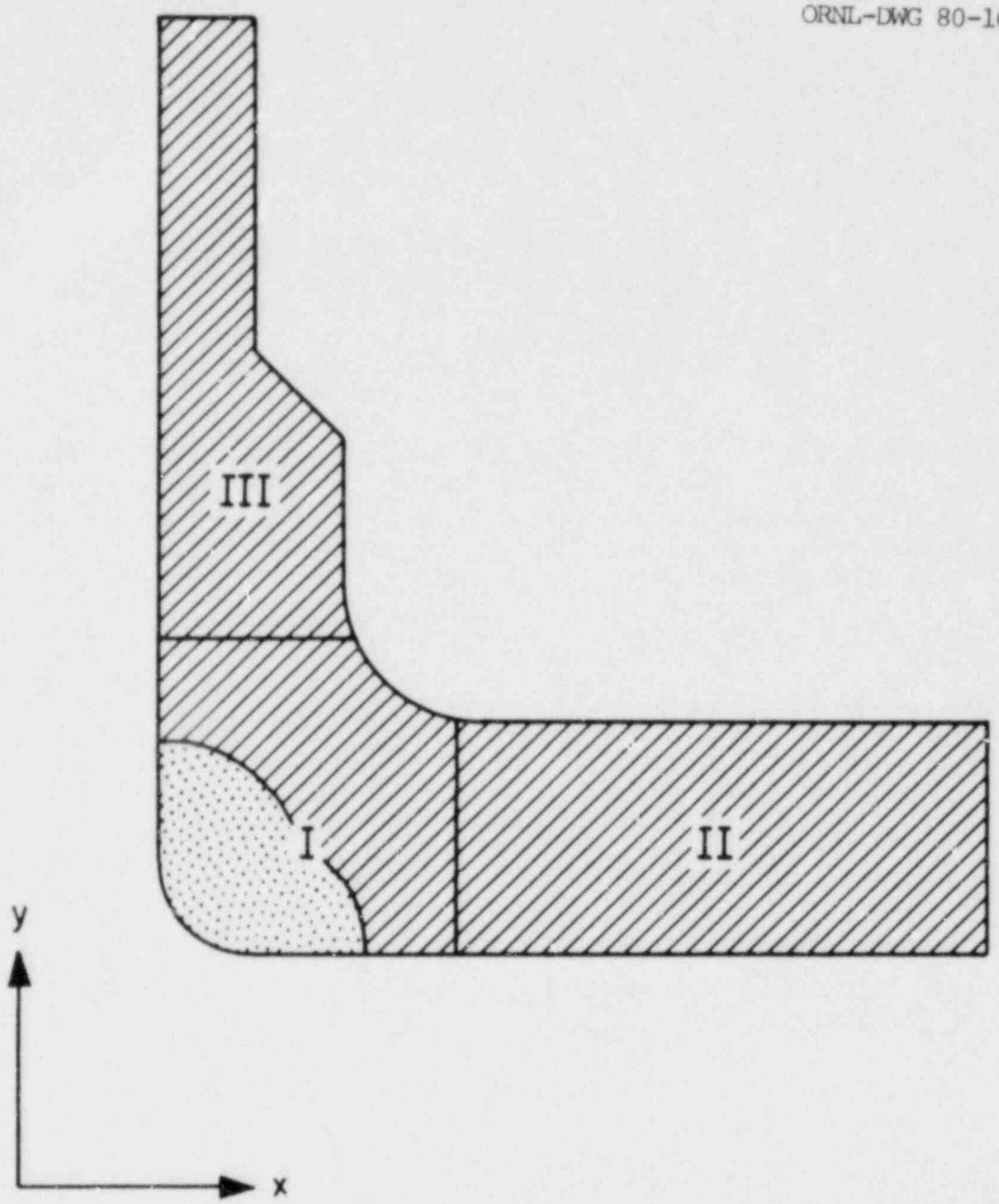

Figure 5. Three regions for AUTO mesh generation

ORNL-DWG 80-16655

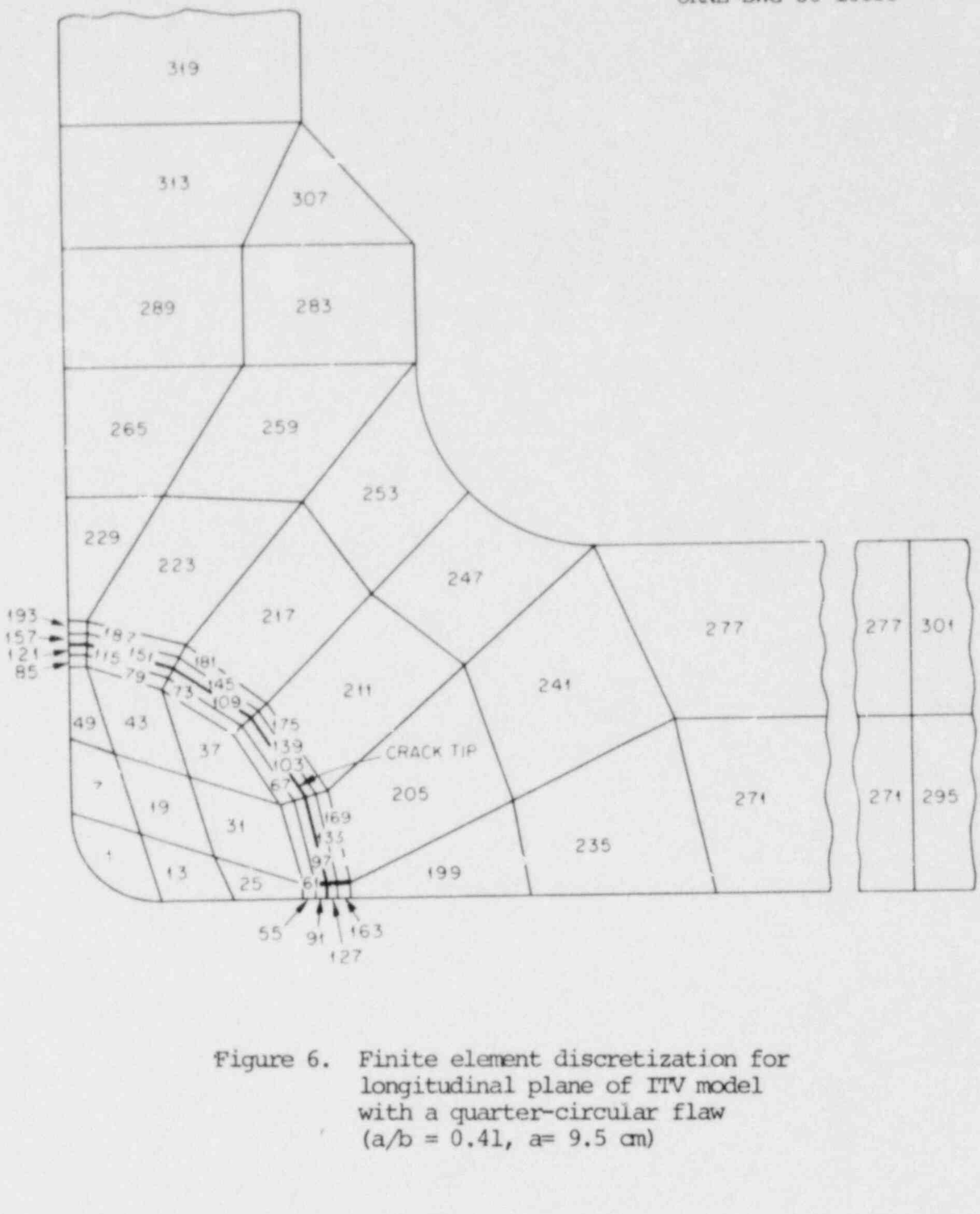

Figure 6. Finite element discretization for longitudinal plane of ITV model with a quarter-circular flaw (a/b = 0.41, a= 9.5 cm)

ORNL-DWG 80-16651

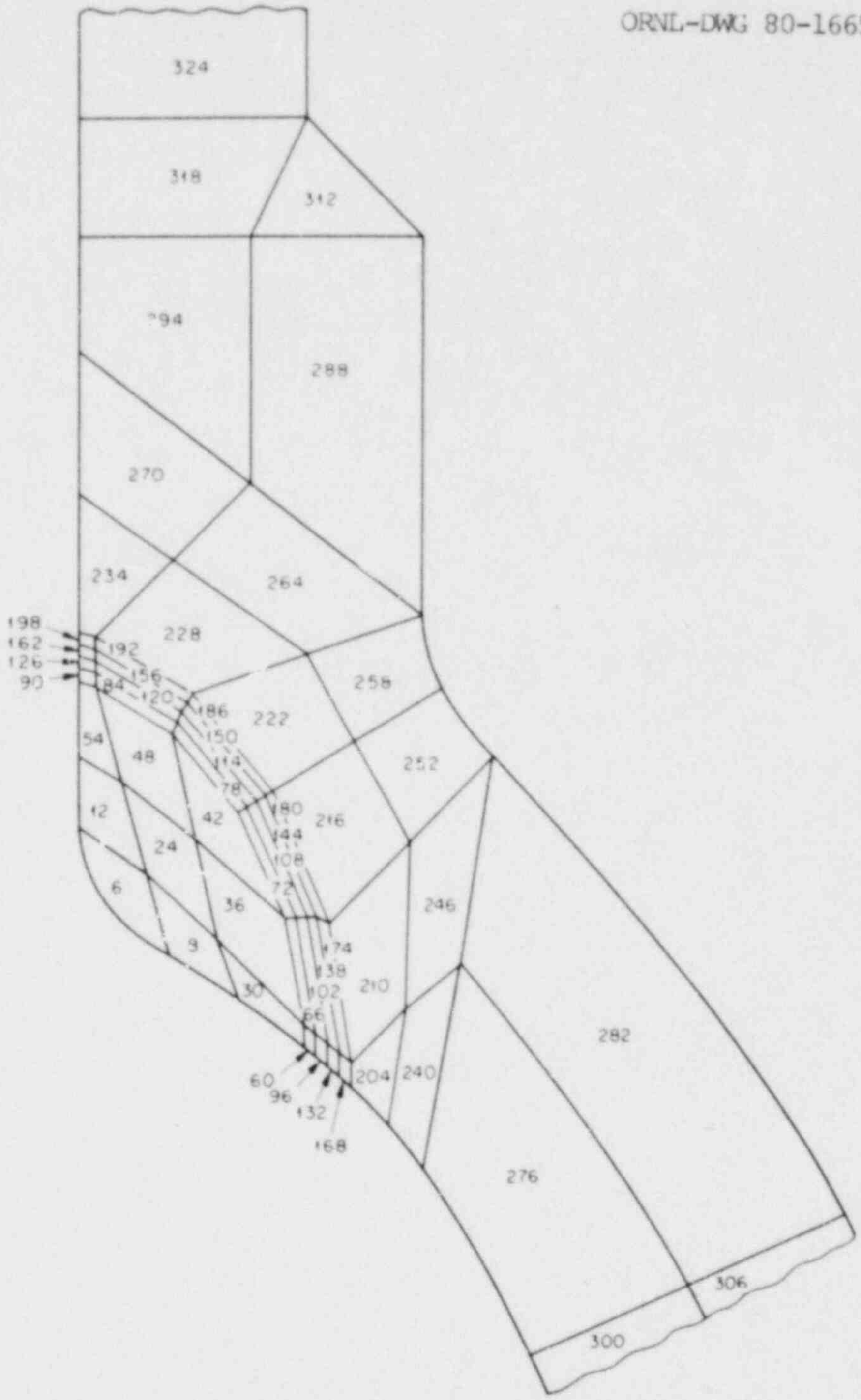

Figure 7. Finite element discretization for transverse plane of ITV model with a quarter-circular flaw (a/b = 0.41, a = 9.5 cm)

ORNL-DWG 80-16641

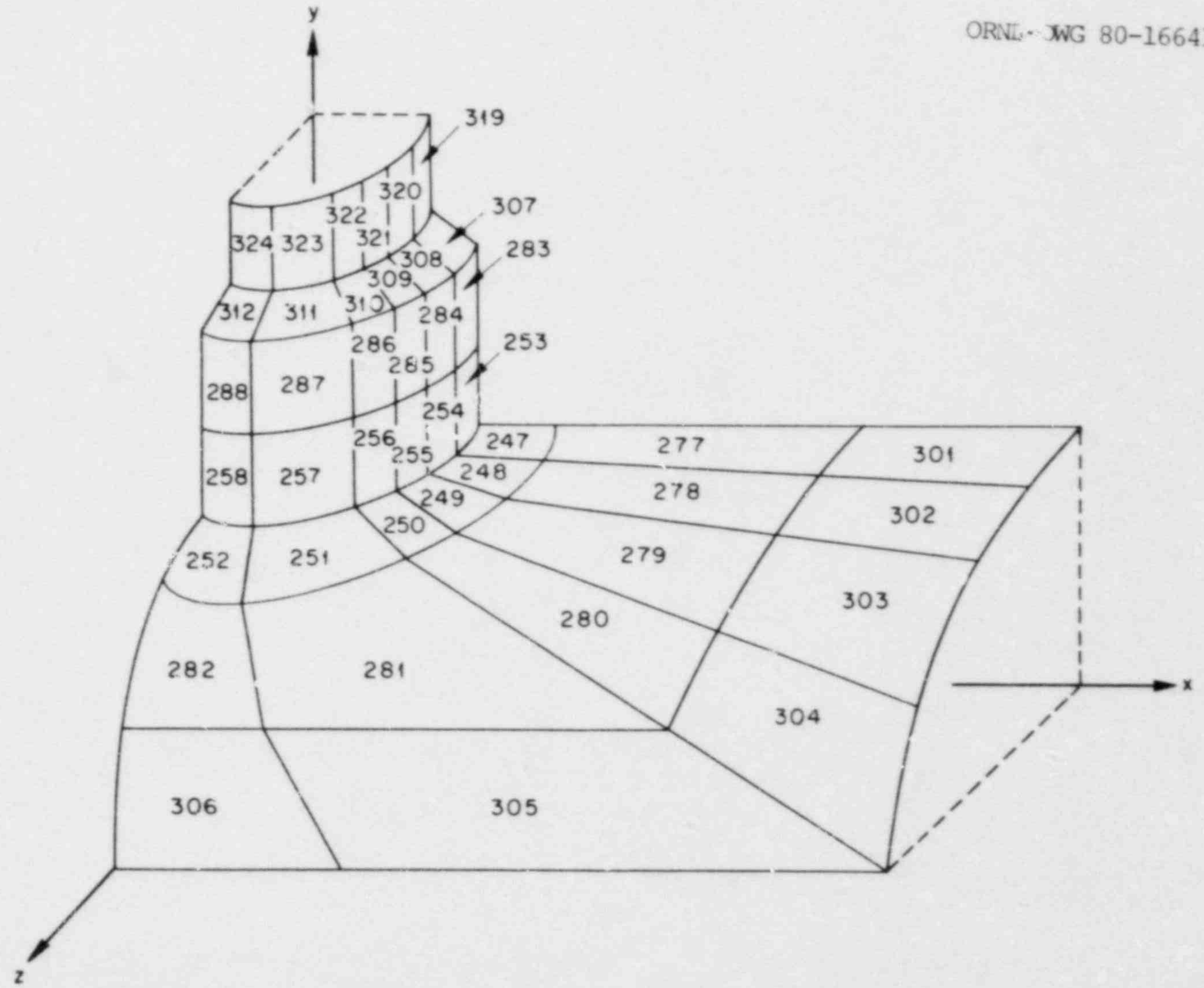

Figure 8. Finite element discretization for outside surface of ITV model with a quarter-circular flaw (not to scale)

ORNL-DWG 80-16640

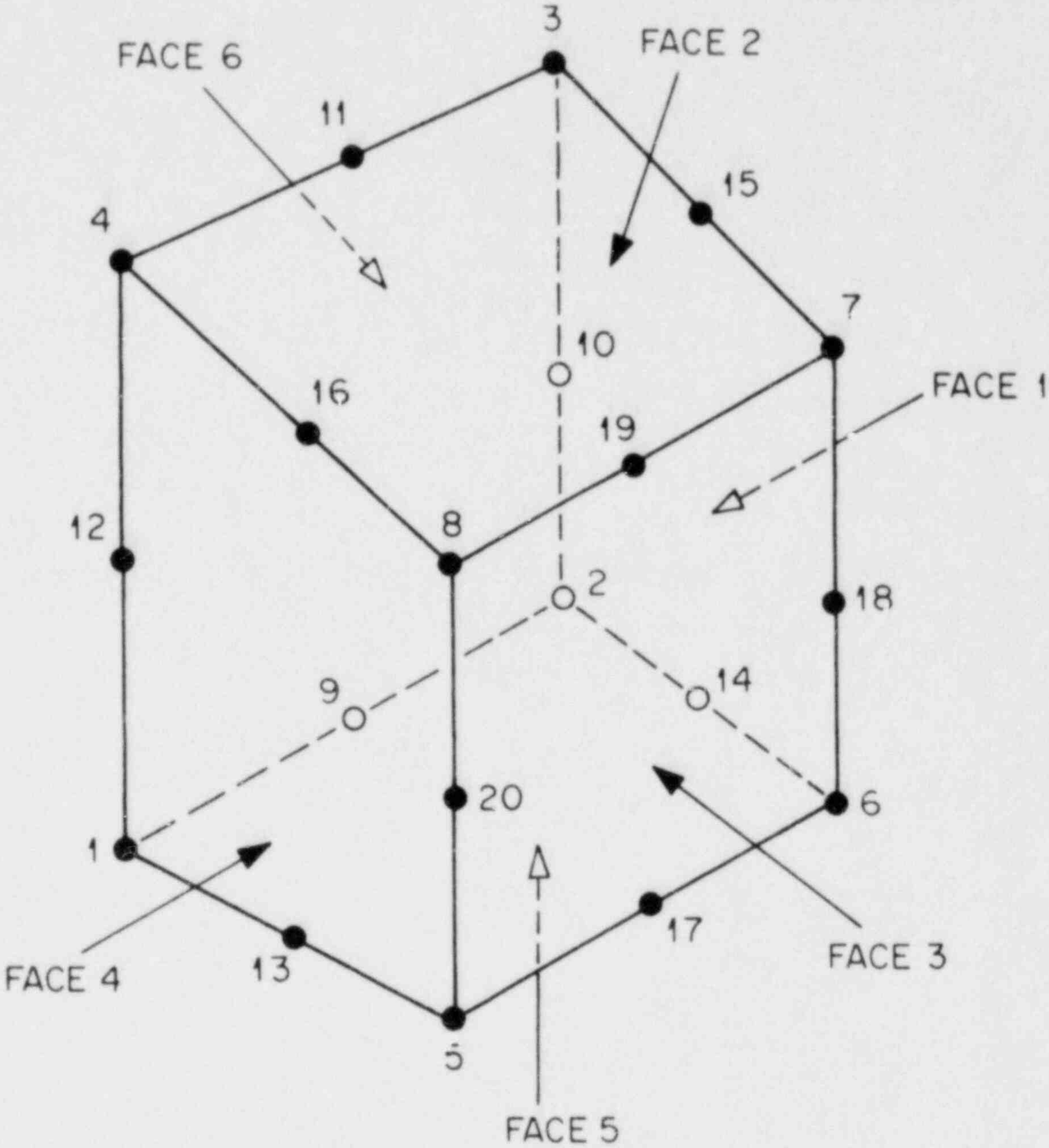

Figure 9. Node and face numbering key for twenty-node isoparameteric brick element

connectivity is dependent upon the location of the element within the model. As shown in Figure 10, the connectivity scheme within the region bounded by the crack tip zone[2] and the nozzle-vessel inner surface is rotated about the y-axis from the longitudinal to the transverse plane. Elements outside this region experience an additional rotation in the nozzle meridional plane, shown in Figure 11.

Program AUTO automatically specifies the appropriate displacement and traction boundary conditions for the symmetric nozzle-vessel configuration shown in Figure 3. In subroutine DSPLBC, nodes in a plane of symmetry are constrained in the direction normal to that plane,[3] except for those nodes in the x-y plane that fall within the crackface. Subroutine TRCBC computes the statically-equivalent node point forces for element faces exposed to internal pressure or end-cap blow-off loads. End caps are simulated by applying equivalent nodal forces to the nozzle and vessel end sections, as shown in Figure 12. Optional fixed-end boundary conditions for the nozzle and vessel are also imposed in this routine.

The instructions generated by program AUTO defining the finite element model are written on a system disk unit[4] to be read later by the solution modules of NOZ-FLAW. In addition, the AUTO-generated instructions are echoed as part of the standard program output to permit the user to verify the finite element model.

---

2 The crack tip zone is that region of the model generated by revolving the four element layers surrounding the crack front about the y-axis from the longitudinal to the transverse plane (see Figure 11).

3 In the output of program AUTO, fixed-displacement boundary conditions are displayed to the user by listing the constrained element faces. The designation "SLOPE = 0" (see microfiche output for example problem, Appendix C) for an element face indicates that each node of the face is constrained in the direction normal to that face.

4 The instructions are written on unit NTAPE2=12.

ORNL-DWG 80-16642

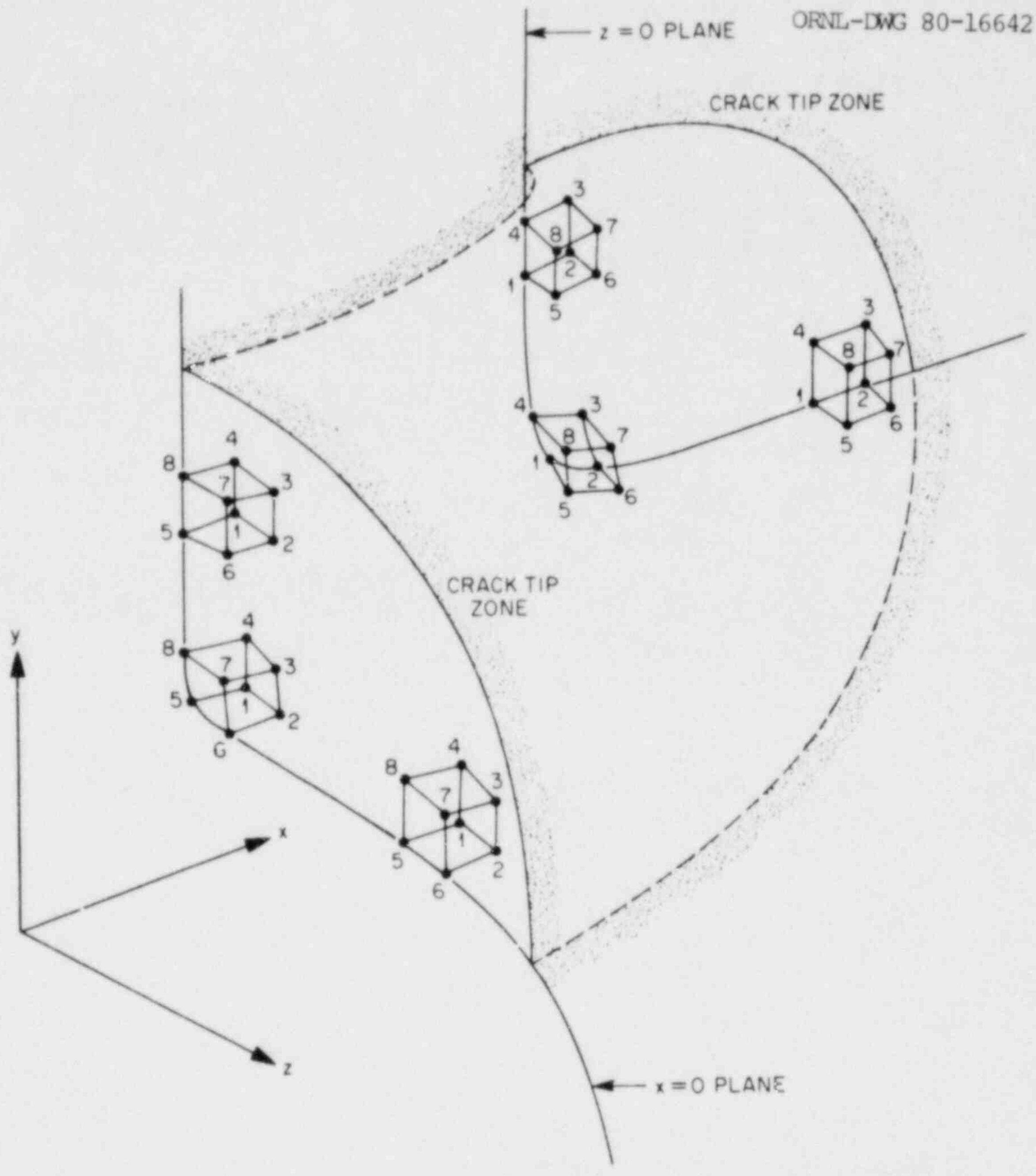

Figure 10. Connectivity orientation for elements in nozzle corner region bounded by the crack tip zone and inner surface

ORNL-DWG 80-16643

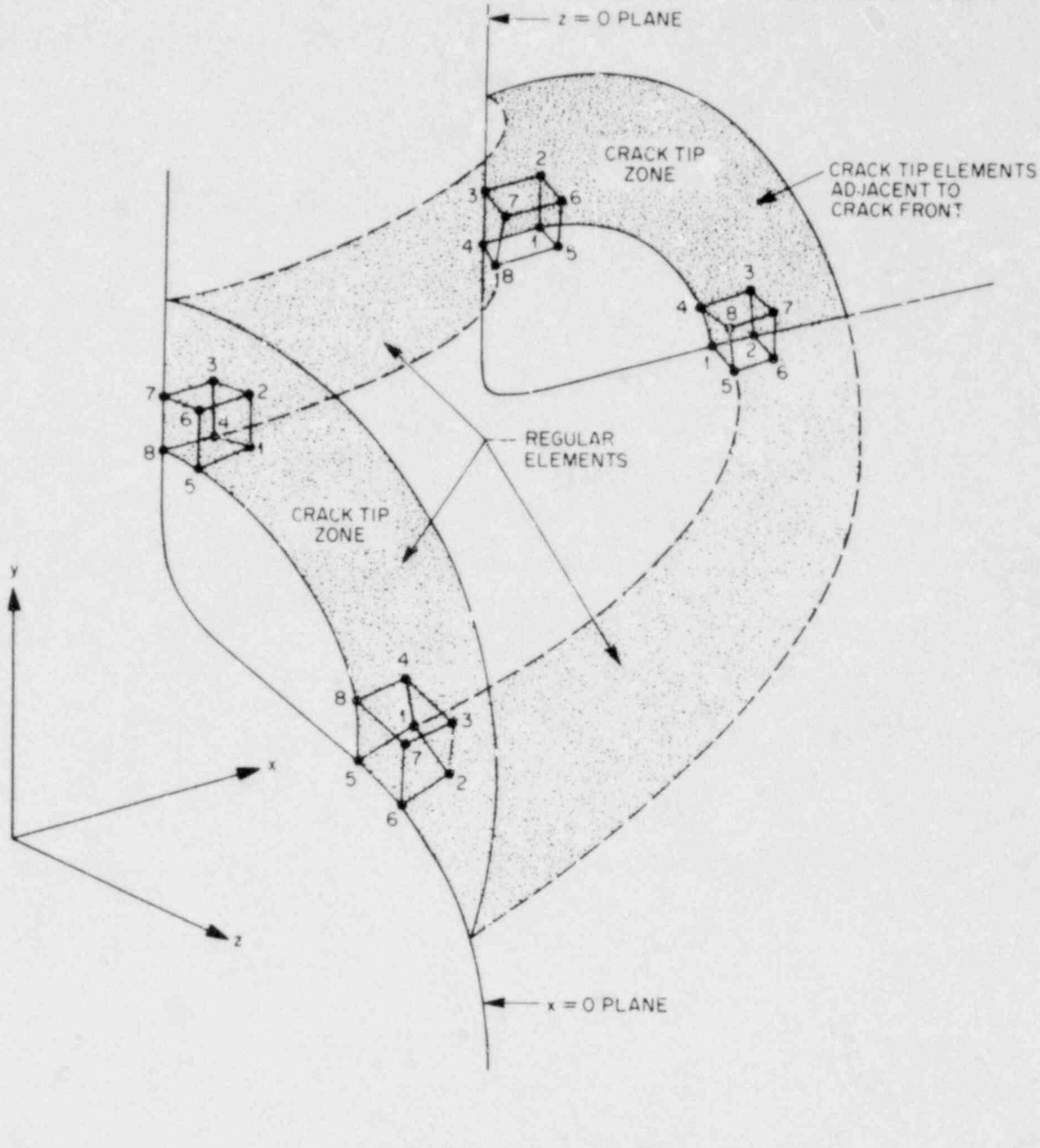

Figure 11. Connectivity orientation for elements in and beyond the crack tip zone

ORNL-DWG 80-16646

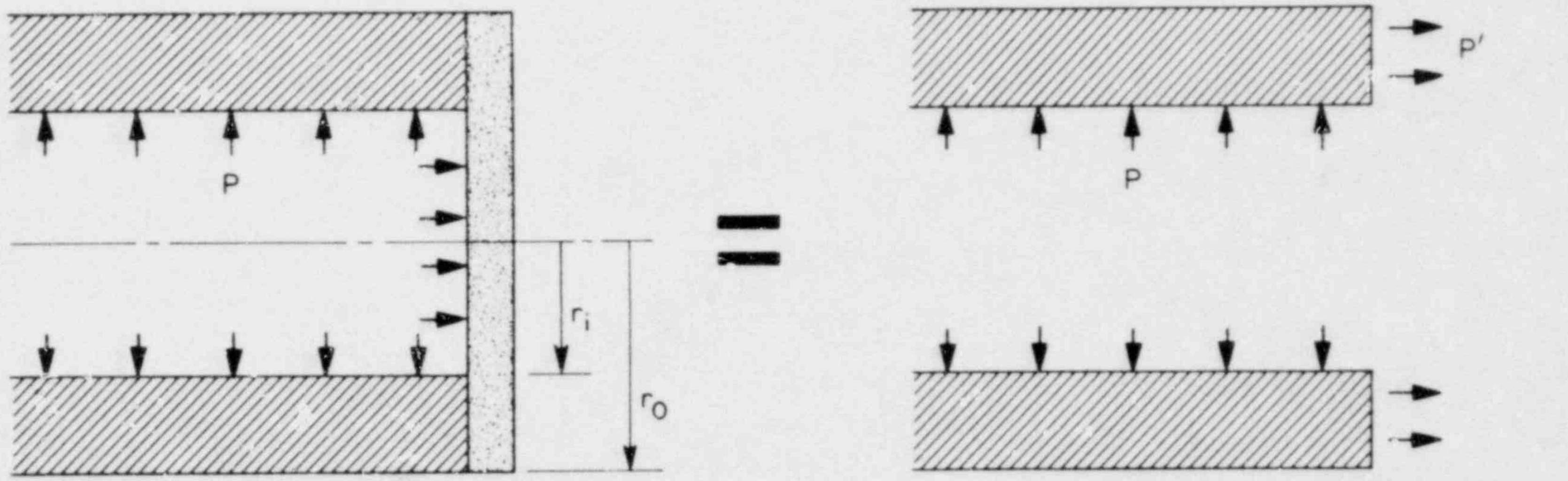

$A = \pi r_i^2$

$A' = \pi (r_o^2 - r_i^2)$

$P' = \frac{PA}{A'} = P\left(\frac{r_i^2}{r_o^2 - r_i^2}\right)$

Figure 12. NOZ-FLAW simulation of nozzle and vessel end caps by application of appropriate end forces F' = P'A'

3. NUMERICAL APPLICATIONS

NOZ-FLAW was used to analyze the intermediate test vessel (ITV) configuration shown in Figure 13. A quarter-circular flaw (MATH) of depth a = 9.5 cm and a similar natural flaw (EXPR) obtained in a photoelastic test [18] were analyzed under internal pressure loading. A crackface pressure equal to the internal pressure (100 MPa) was applied simultaneously. For comparison purposes, the quarter-circular flaw was also analyzed under internal pressure loading without crackface pressure. Figures 6 and 7 show longitudinal and transverse cross sectional views of the finite element mesh generated by NOZ-FLAW for the quarter-circular flaw model. Top and side views of the outside surface of the mesh are also given in Figures 14 and 15. A total of 324 elements and 1791 nodes was generated for this model.

The results of the analyses are shown in Figure 16, where normalized K_I values are given at various points along the flaw front measured from the vessel free surface. The NOZ-FLAW values were obtained by averaging K-values from corresponding crack tip elements on each side of the crack. In addition, results are presented for the quarter-circular flaw using the BIGIF [27] computer program. BIGIF uses an influence function approach for the calculation of K-values and requires a prior stress analysis of the uncracked structure. This stress analysis was obtained using the CORTES-EP [28] finite element program. Each of the three NOZ-FLAW analyses, as well as the BIGIF analysis, gave K_I distributions with relative maximums near the free surfaces and a relative minimum near the 45 position. The photoelastic results, however, show an opposite trend. It should be pointed out that these tests were conducted on small scale epoxy models which actually had the back free surface configuration indicated by the dotted boundary in Figure 13. Also, the inner nozzle corner fillet radius of the photoelastic models was slightly smaller than that modeled by NOZ-FLAW. One can also observe from Figure 16 that the inclusion of crackface pressure significantly elevates the NOZ-FLAW calculated K-values.

Each of the NOZ-FLAW analyses required 1200K of memory and approximately 28 minutes of CPU time on the UCC-ND IBM 360/195. The input for each of the analyses shown is listed in Appendix C. A complete output from NOZ-FLAW for the quarter-circular flaw with crackface pressure is given on microfiche and attached to the back cover (see Appendix C).

ORNL-DWG 80-16644

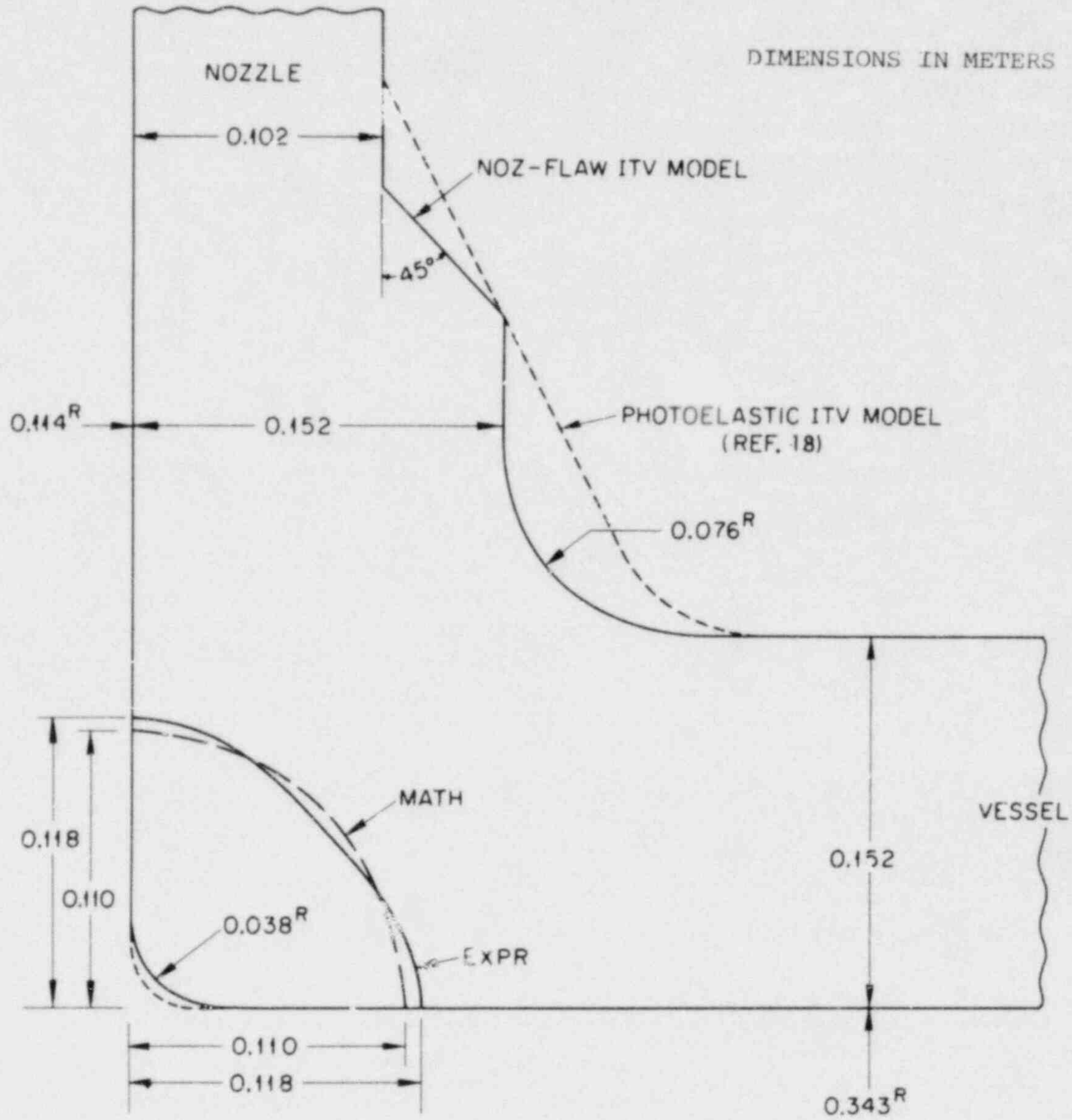

Figure 13. Geometry and dimensions of an ITV configuration

ORNL-DWG 80-16649

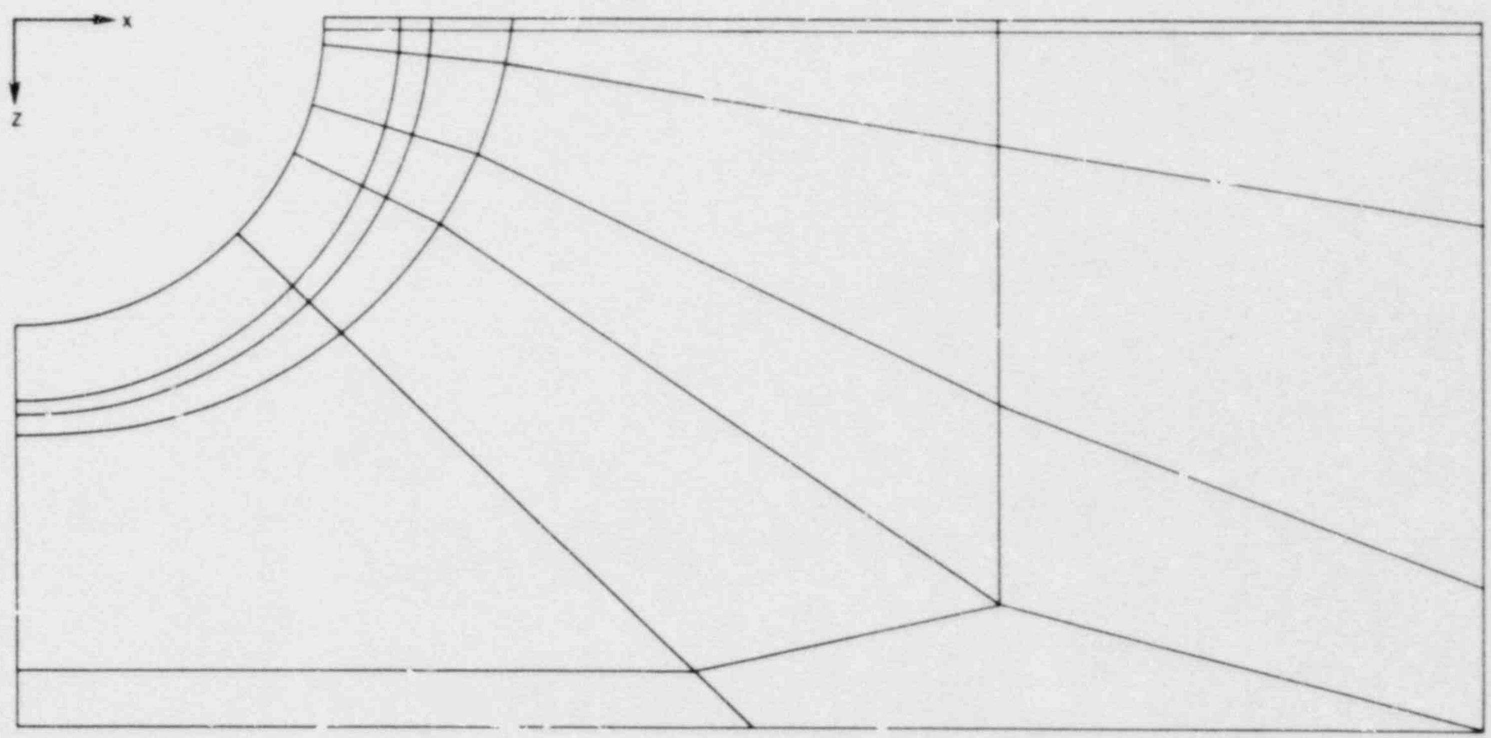

Figure 14. Top view (normal to x-z plane) of outside surface of finite element mesh generated by NOZ-FLAW for ITV configuration

ORNL-DWG 80-16650

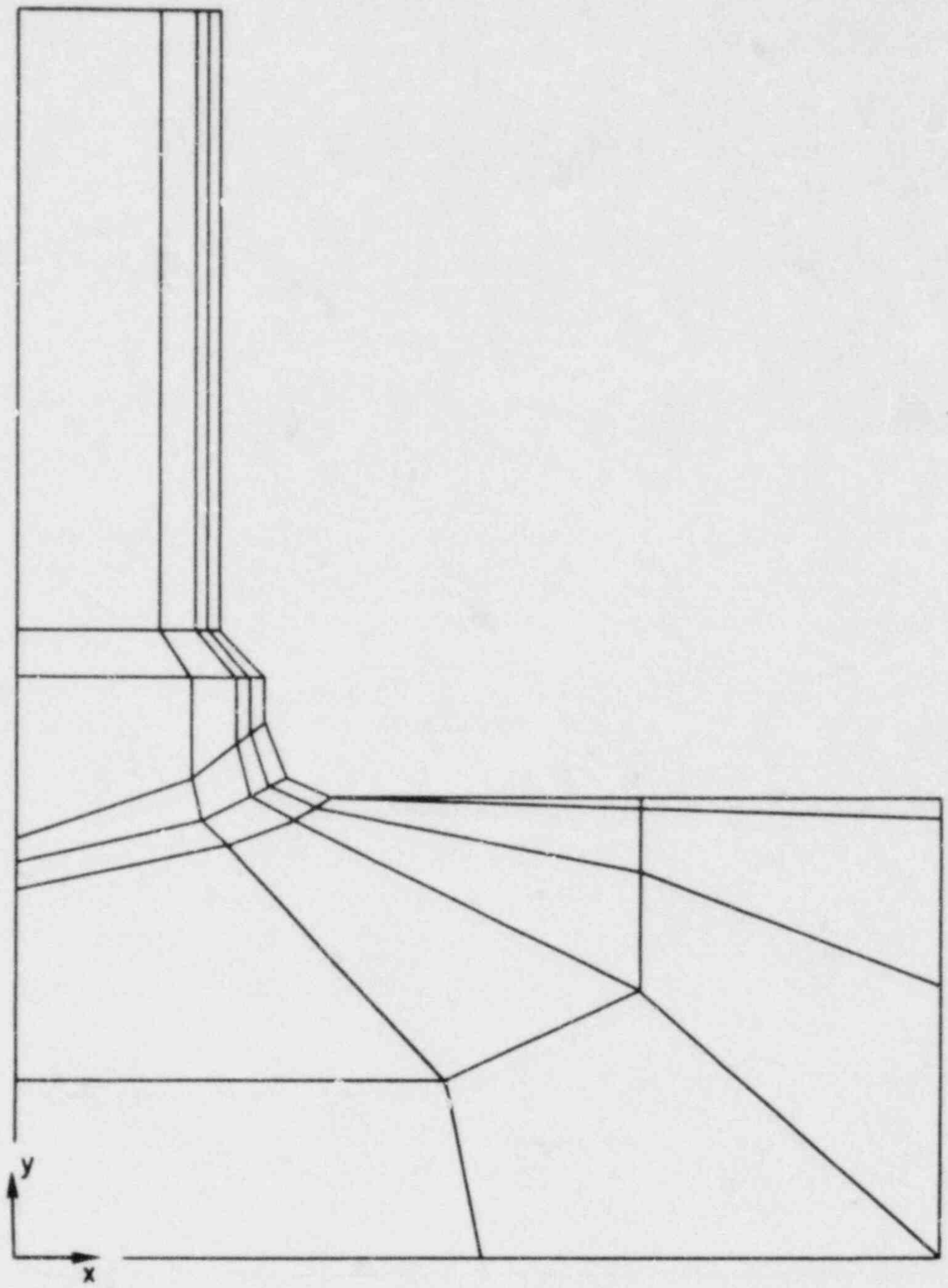

Figure 15. Side view (normal to x-y plane) of outside surface of finite element mesh generated by NOZ-FLAW for ITV configuration

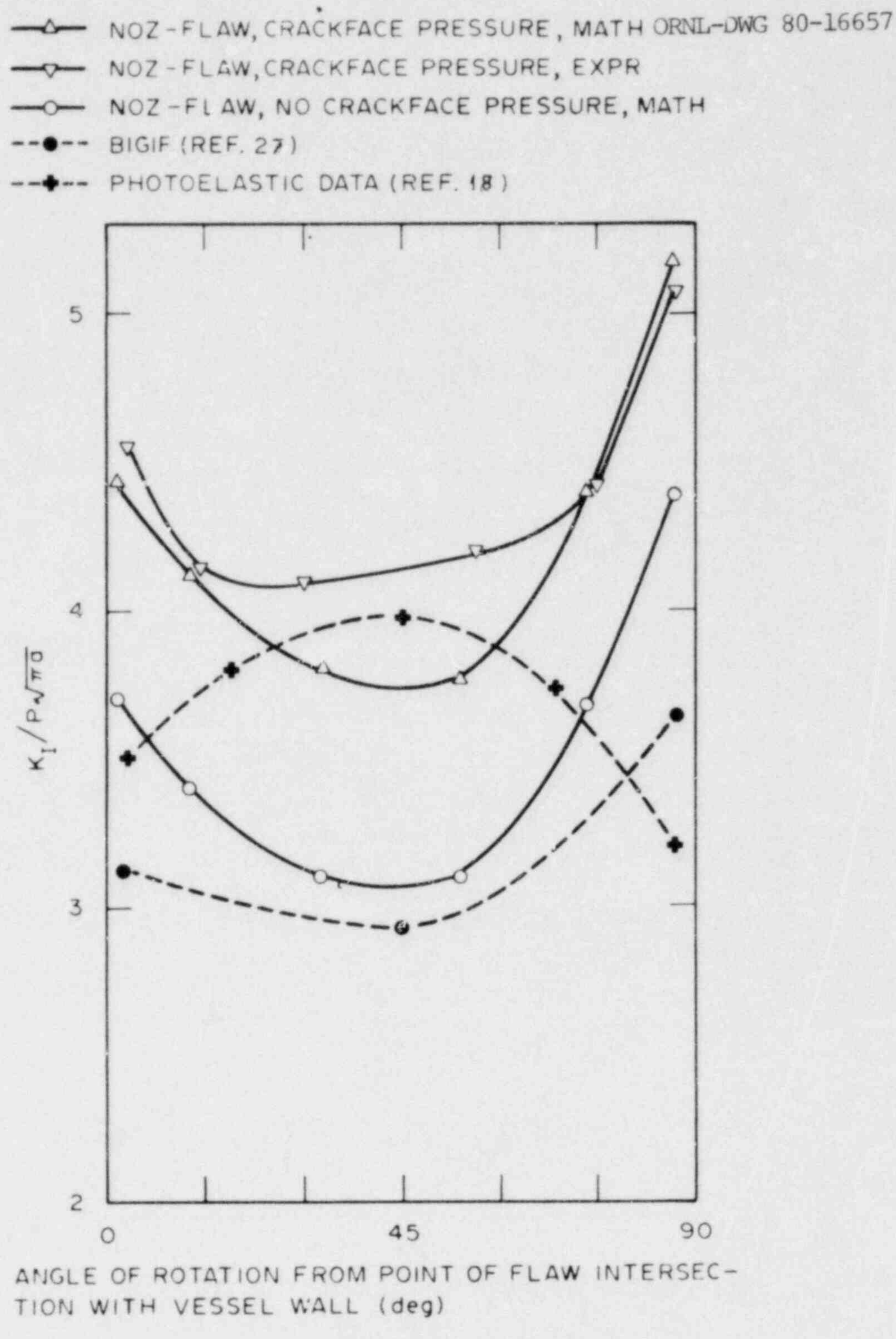

Figure 16. Variation of K_I along a quarter-circular flaw and experimentally measured flaw (Ref. 18) in an ITV configuration (a/b = 0.41, a = 9.5 cm)

4. CONCLUSIONS

NOZ-FLAW is a linear elastic finite element computer program which calculates nozzle corner flaw stress intensity factors. Unique features include the use of special crack tip elements (hybrid-displacement), direct calculation of K-values, and automatic mesh generation incorporating user-defined crack flaws. As few as eight cards of input are required to automatically generate a finite element model and to execute the program. The convenience of limited input, however, introduces certain limitations or restrictions. The flaw must be positioned in the longitudinal plane of a standard reinforced pressure vessel nozzle configuration. Only internal pressure loading, with or without crackface pressure, may be considered. A finite element mesh is generated and appropriate boundary conditions are imposed for one-eighth of a configuration that possesses threefold symmetry. Thus, use of the present version of NOZ-FLAW to analyze a single nozzle with a single flaw ignores the effects of a second nozzle underneath the vessel as well as the additional flaws remote from the flaw of interest. It is therefore recommended that NOZ-FLAW be used only for relatively small-diameter nozzles attached to relatively large-diameter vessels. Also, the size of the special crack tip elements should be no more than one-tenth of the flaw depth.

Minor modifications of the NOZ-FLAW mesh generator will permit the analysis of a nozzle corner flaw configuration with two planes of symmetry, i.e., the second nozzle underneath the vessel could be removed. Other loadings could be considered by modifying the boundary condition routines. Work is currently under way to develop a more general program for the analysis of user-defined crack flaws in flat plates, cylinders, and nozzle corners. Other future developments include the addition of thermal loading and graphics plotting routines to the expanded version of the program.

ACKNOWLEDGMENTS

The NOZ-FLAW computer program was initiated under the direction of Professor S. N. Atluri, School of Engineering Science and Mechanics, Georgia Institute of Technology. The work was sponsored by the Heavy Section Steel Technology Program (HSST) under UCC-ND Subcontract 7565 between UCC-ND and Georgia Institute of Technology.

The authors gratefully acknowledge the assistance of W. G. Johnson and J. B. Drake, UCC-ND Computer Sciences Division, in setting up the program to operate on the UCC-ND computer facilities. Special thanks are due R. H. Bryan, ORNL, who provided much encouragement in addition to his many technical contributions in this work.

Finally, the authors wish to express their gratitude to L. W. Walker for typing the drafts and preparation of the manuscript.

REFERENCES

1. A. G. Pickett and S. C. Grigory, Trans. ASME Journal of Basic Engineering 89(c), 858-870 (December 1967).

2. K. E. Stahlkopf, R. E. Smith, and T. U. Marston, Nuclear Engineering and Design 46(1), 65-79 (March 1978).

3. J. F. Knott, Fundamentals of Fracture Mechanics, John Wiley and Sons, New York, 1973.

4. S. Yukawa, Evaluation of Periodic Proof Testing and Warm Prestressing Procedures for Nuclear Reactor Vessels, HSSTP-TR-1 (July 1, 1969).

5. P. C. Paris and G. C. Sih, "Stress Analysis of Cracks," pp. 30-83 in Fracture Toughness Testing and Its Applications, ASTM STP 381, American Society for Testing and Materials, 1965.

6. F. W. Smith, "Stress Intensity Factors for a Semi-Elliptical Surface Flaw," Structural Development Research Memorandum No. 17, Boeing Company, Seattle, Washington, August 1966.

7. J. Gilman and Y. Rashid, "Three-Dimensional Analysis of Reactor Pressure Vessel Nozzles," Paper G2/6, First International Conference on Structural Mechanics in Reactor Technology, Berlin, 1971.

8. J. Reynen, "Analysis of Cracked Pressure Vessel Nozzles by Finite Elements," Paper G5/1, Third International Conference on Structural Mechanics in Reactor Technology, London, 1975.

9. T. Hellen and A. Dowling, "Three-Dimensional Crack Analysis Applied to an LWR Nozzle-Cylinder Intersection," International Journal of Pressure Vessels and Piping, Vol. 3, pp. 57-74, 1975.

10. M. Broekhaven, "Computation of Stress Intensity Factors for Nozzle Corner Cracks by Various Finite Element Procedures," Paper G4/6, Third International Conference on Structural Mechanics in Reactor Technology, London, 1975.

11. W. Schmitt et al., "Calculation of Stress Intensity Factors for Cracks in Nozzles," International Journal of Fracture, Vol. 12, 1976, pp. 381-390.

12. S. N. Atluri and K. Kathiresan, "Influence of Flaw Shapes on Stress Intensity Factors for Pressure Vessel Surface Flaws and Nozzle Corner Cracks," ASME Pressure Vessels and Piping Conference, 79-PVP-65, San Francisco, California, June 25-29, 1979.

13. A. Kobayashi et al., "Stress Intensity Factors of Corner Cracks in Two Nozzle-Cylinder Intersections," Paper G4/4, Fourth International Conference on Structural Mechanics in Reactor Technology, San Francisco, California, 1977.

14. P. Besuner, L. Cohen, and J. McLean, "The Effects of Location, Thermal Stress, and Residual Stress on Corner Cracks in Nozzles with Cladding," Paper G4/5, Fourth International Conference on Structural Mechanics in Reactor Technology, San Francisco, California, 1977.

15. P. Besuner and W. Caughey, "Comparison of Finite Element and Influence Function Methods for Three-Dimensional Elastic Analysis of Boiling Water Reactor Feedwater Nozzle Cracks," Reactor Feedwater Nozzle Cracks," EPRI NP-261, November 1976.

16. M. A. Mohamed and J. Schroeder, "Stress Intensity Factor Calculations for Circular Cracks at the Intersections of Pressurized Cylindrical Shells," 78-PVP-24, Joint ASME/CSME Pressure Vessels and Piping Conference, Montreal, Canada, June 25-30, 1978.

17. R. Derby, "Shape Factors for Nozzle-Corner Cracks," Experimental Mechanics, Vol. 12, 1972, pp. 580-584.

18. C. W. Smith, M. Jolles, and W. H. Peters, Stress Intensities for Nozzle Cracks in Reactor Vessels, VPI-E-76-25, ORNL/SUB-7015/1, Virginia Polytechnic Institute and State University, November 1976.

19. C. W. Smith, et al., Stress Intensity Distributions in Nozzle Corner Cracks of Complex Geometry, VPI-E-79-2, NUREG/CR-0640,ORNL/SUB/7015-2, Virginia Polytechnic Institute and State University, January 1979.

20. K. Kathiresan, "Three-Dimensional Linear Elastic Fracture Mechanics Analysis by a Displacement Hybrid Finite Element Model," Ph.D. Dissertation, School of Engineering Science and Mechanics, Georgia Institute of Technology, Atlanta, Georgia, September 1976.

21. S. N. Atluri, K. Kathiresan, and A. S. Kobayashi, "Three-Dimensional Linear Fracture Mechanics Analysis by a Displacement-Hybrid Finite Element Model," Paper L7/3, Third International Conference on Structural Mechanics in Reactor Technology, London 1975.

22. E. B. Becker and R. S. Dunham, TEXGAP3D: User Oriented Three-Dimensional Static Linear Elastic Stress Analysis Program, Texas Institute for Computational Mechanics, University of Texas at Austin, March 1977.

23. S. N. Atluri and K. Kathiresan, "Outer and Inner Surface Flaws in Thick-Walled Pressure Vessels," Paper G5/4, Fourth International Conference on Structural Mechanics in Reactor Technology, San Francisco, California, August 1977.

24. S. N. Atluri and K. Kathiresan, "3-D Analyses of Surface Flaws in Thick-Walled Reactor Pressure Vessel Using Displacement-Hybrid Finite Element Method," Nuclear Engineering and Design, Vol. 15, No. 2, January 1979, pp. 163-176.

25. S. N. Atluri and K. Kathiresan, "Stress Intensity Factor Solutions Arbitrarily Shaped Surface Flaws in Reactor Pressure Vessel Nozzle Corners," Paper G4/3, Fifth International Conference on Structural Mechanics in Reactor Technology, Berlin, August 1979.

26. F. K. W. Tso, et al., Stress Analysis of Cylindrical Pressure Vessels with Closely Spaced Nozzles by the Finite-Element Method, Vol. 1. Stress Analysis of Vessels with Two Closely Spaced Nozzles Under Internal Pressure, ORNL/NUREG-18/V1, Oak Ridge National Laboratory, Oak Ridge, Tennessee, November 1977.

27. P. M. Besuner, D. C. Peters, and R. C. Cipolla, BIGIF: Fracture Mechanics Code for Structures, NP-838, Failure Analysis Associates, July 1978.

28. G. H. Powell, Finite Element Analysis of Elasto-Plastic Tee Joints, UC SESM 74-14, ORNL/SUB/3193-2, Department of Civil Engineering, University of California, Berkeley, September 1974.

APPENDICES

APPENDIX A

NOZ-FLAW INSTRUCTIONS

NOZ-FLAW requires as few as eight input cards to generate a finite element mesh and to execute an analysis. The program permits free format input for all but the first card, where AUTO must be specified in columns 1-4. Variable values are separated by commas and blanks are ignored, i.e., NO ZZLE will be read as NOZZLE. Cards C-H must end with a $ and card B must begin with a $. A / is used to continue data to the next line, for example:

```
5, 5, 3/          Line 1
2, 5              Line 2
```

is the same as

```
5, 5, 3, 2, 5     Line 1 .
```

If a variable is zero or if the user chooses not to specify a variable, two consecutive commas (,,) may be used. For example:

```
5,5,, 2, 5
```

is the same as

```
5, 5, 0, 2, 5 .
```

A comma should not be used before a / unless the last variable value is zero. For example,

```
5, 5, 3, /

2, 5
```

is not the same as

```
5, 5, 3, 2, 5 .
```

The program would interpret this as

```
5, 5, 3, 0, 2, 5 .
```

Finally, integer variables should receive integer values. Real variables require decimal input. For example, input for Card E with parameters NX1, NX2, NX3, NX4, NY1, NY2, NZ, SIZE, GRADX might be 2, 2, 2, 1, 1, 2, 4, 0.005, 1.5$.

INPUT DATA

CARD A. Mesh generation code - specify AUTO in columns 1-4.

CARD B. Title - A $ must appear in column 1. Any symbol other than a / may appear in columns 2-80.

CARD C. Parameters PBTPE, E, PO, CRACK, PMODEL. End this card with a $.

PBTPE - Specify NOZZLE
E - Young's modulus for material
PO - Poisson's ratio for material
CRACK - Specify NDCORNER*
PMODEL - Specify 0.125*

*These values instruct NOZ-FLAW to generate a finite element mesh for the threefold symmetric configuration shown in Figure 3. Other mesh generation options are planned.

CARD D. Parameters CRPRF, PVR, PVT, PNR, PNT, PVL, PNL, R1, R2, PNL1, PNL2, PNT2, NCRS. End this card with a $. See Figure 17 for a definition of these variables.

CRPRF - Specify MATH or EXPR; MATH for quarter-circular or quarter-elliptical flaws, EXPR for user-defined crack flaws.

PVR - Pressure vessel inner radius
PVT - Pressure vessel thickness
PNR - Nozzle inner radius
PNT - Nozzle thickness above reinforcement
PVL - Pressure vessel length
PNL - Nozzle length
R1 - Inner fillet radius
R2 - Outer fillet radius
PNL1 - Nozzle length above reinforcement
PNL2 - Nozzle length to reinforcement
PNT2 - Nozzle thickness at reinforcement
NCRS - Number of mesh divisions along crack front

NOTE: $NCRS \geq NY1 + NY2 + 2$ (see CARD E)

ORNL-DWG 16656

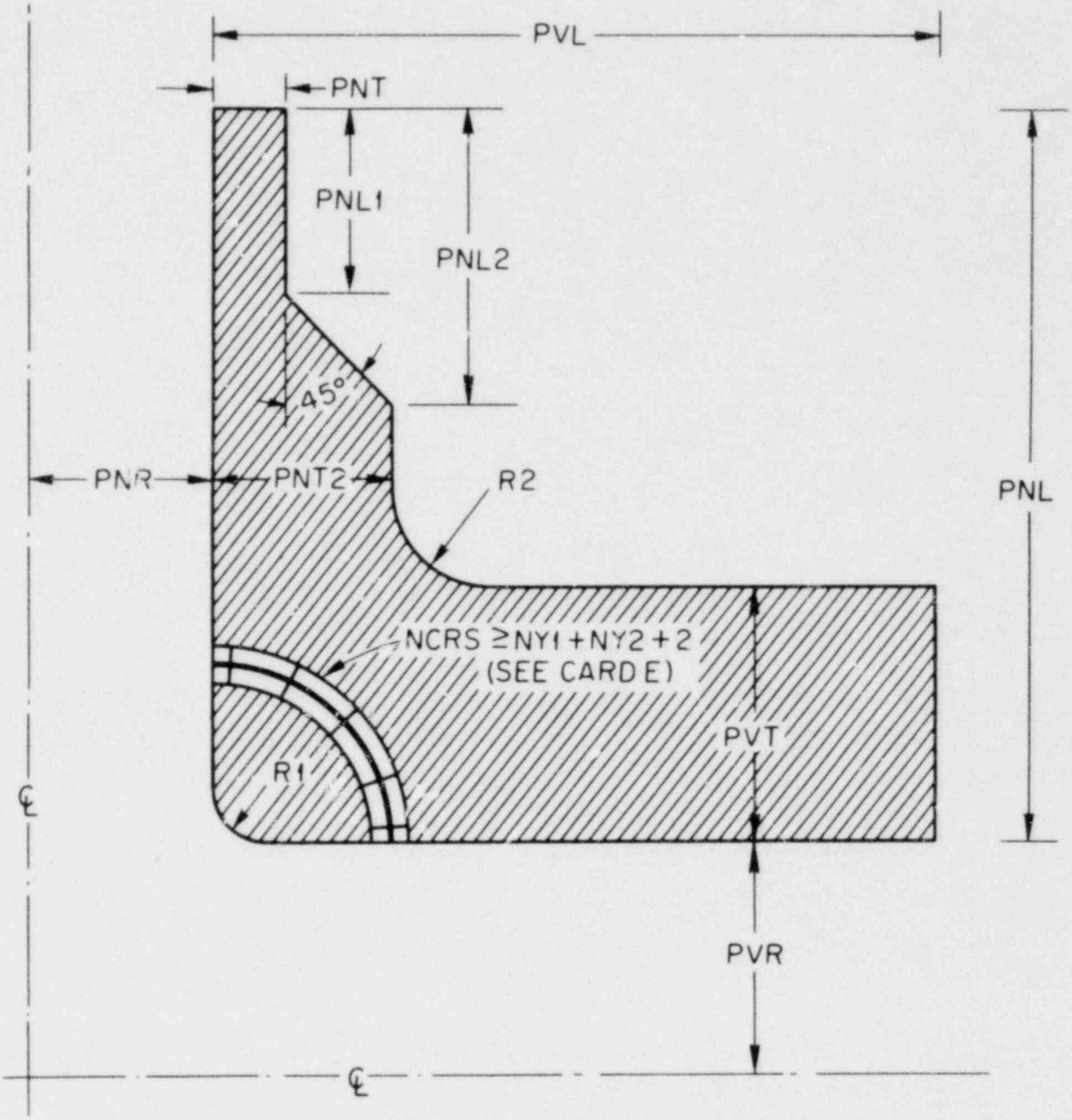

Figure 17. Dimensional parameters for nozzle corner flaw configuration

CARD E. Mesh division parameters NX1, NX2, NX3, NX4, NY1, NY2, NZ, SIZE, GRADX. End the card with a $. See Figure 18 for a definition of these variables.

NOTE: NX3 $\geq$ NCRS - NY1 - NY2 - 2

CARD F. Crack definition. End this card with a $.

For CRPRF = MATH on CARD D, input CRA, CRB. See Figure 19 for a definition of these variables.

For CRPRF = EXPR, input X(I), I=1, 2*NCRS+1, 2
Y(I), I=1, 2*NCRS+1, 2

See Figure 20 for a definition of these variables.

NOTE 1: X_i and Y_i should be input using the local coördinate system shown in Figure 20.

NOTE 2: (PNR + CRA + 2 * SIZE) < 0.95 * PVR (for MATH)
or
(PNR + X(1) + 2 * SIZE) < 0.95 * PVR (for EXPR)

CARD G. Pressure loading and boundary conditions. End this card with a $.

Possible inputs are:

CYPRESS, P
CRPRESS, P
ENDCAP, P
ENDDSPL

CYPRESS, P - Application of uniform internal pressure of magnitude P in both cylinder and nozzle.

CRPRESS, P - Application of uniform pressure of magnitude P on the crack surface.

ENDCAP,P - Simulates end caps by applying appropriate force loadings at nozzle and cylinder end nodes. P is the internal pressure loading. See Figure 12.

ENDDSPL - Suppresses axial displacements at nozzle and cylinder ends. May not be specified simultaneously with ENDCAP,P.

ORNL-DWG 80-16654

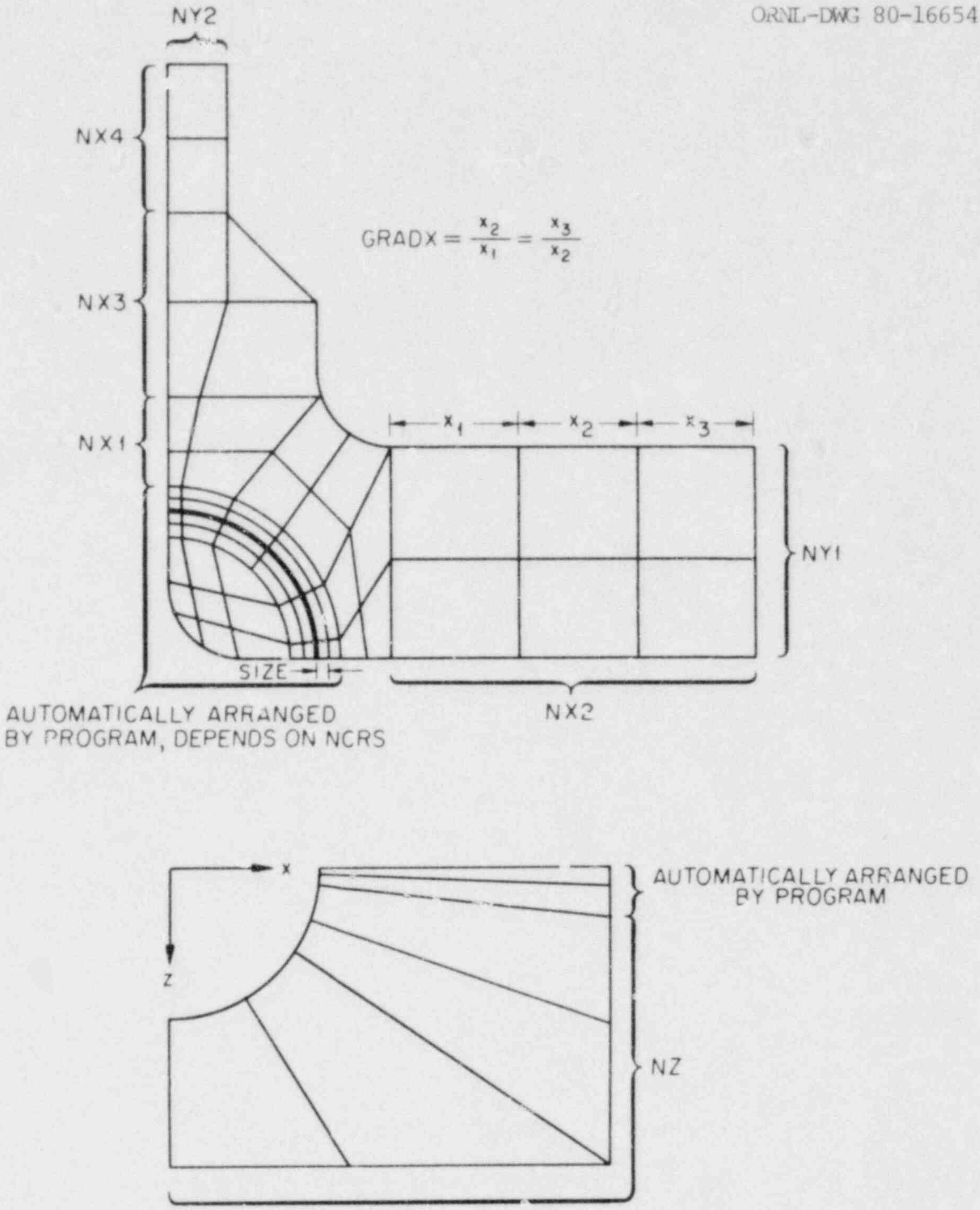

Figure 18. Mesh generation parameters for nozzle corner flaw configuration

ORNL-DWG 80-16652

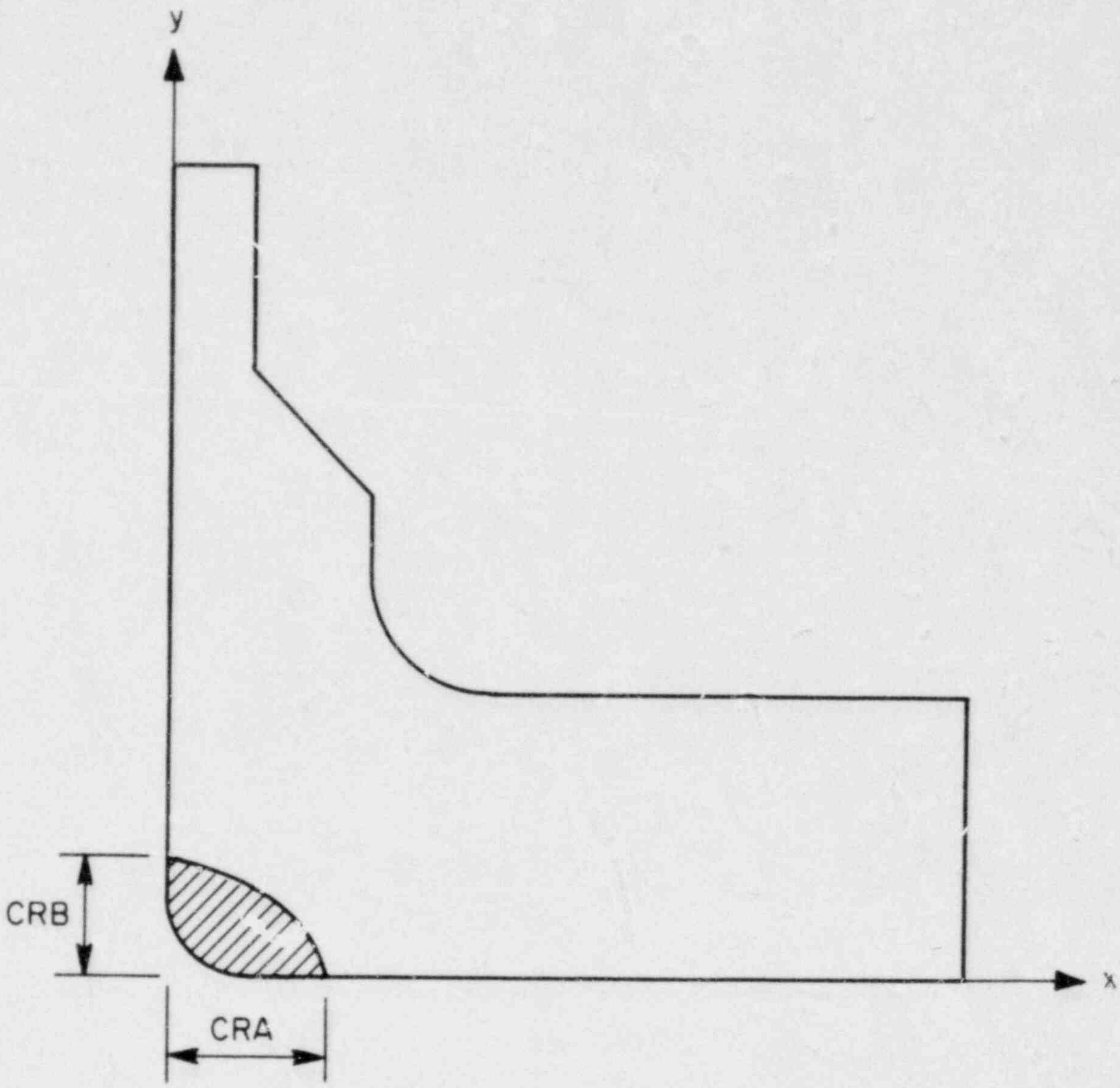

Figure 19. Crack definition parameters

ORNL-DWG 80-16653

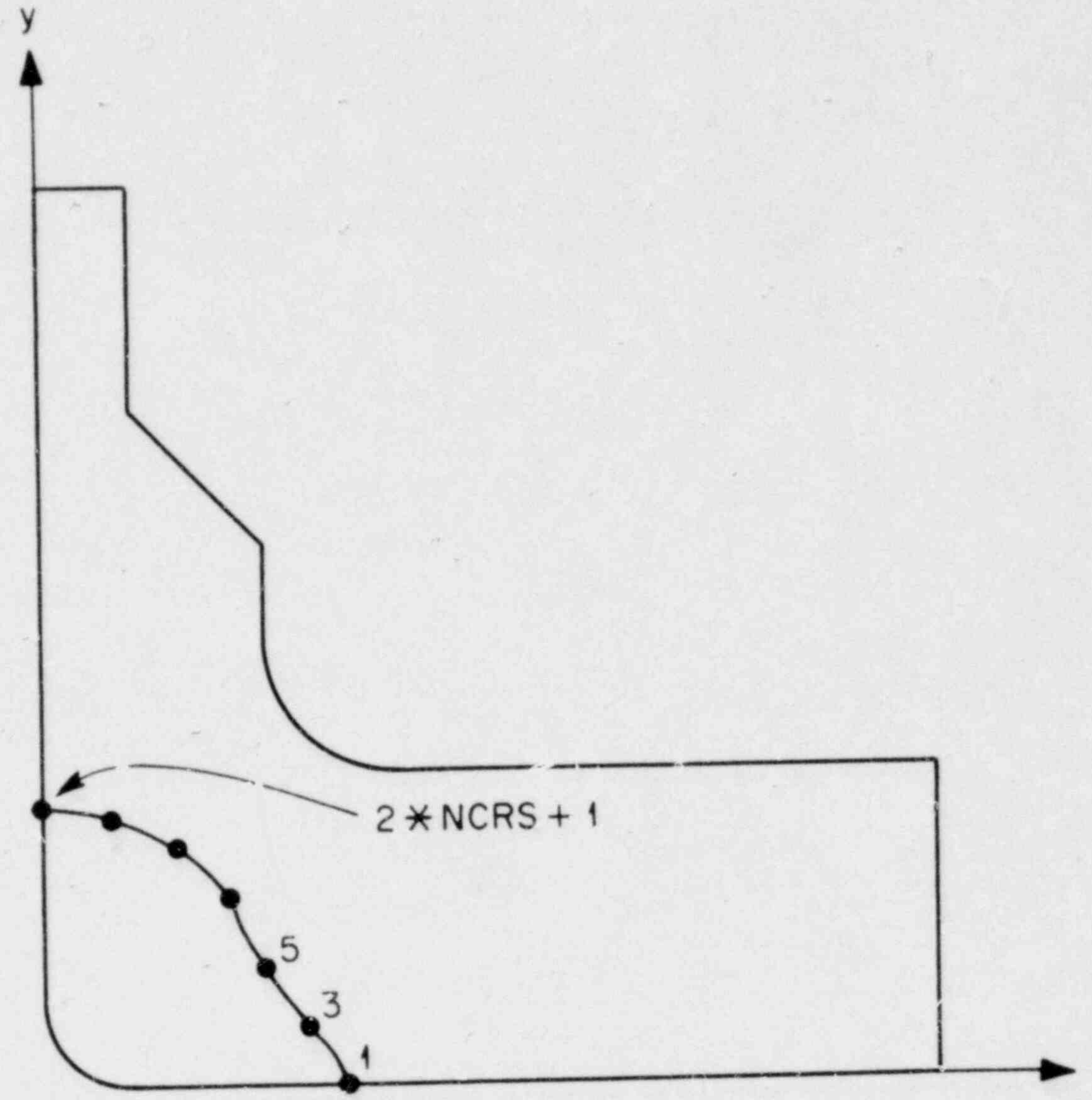

Figure 20. Local coordinate definition of crack front for CRPRF = EXPR

CARD H. Termination and printout option. End this card with a $.

End of input is signaled by specifying ENDBC. Stress intensity factors as well as stresses, strains, and displacements for the entire structure are printed. If only the stress intensity factors are desired, then specify SIF following ENDBC.

Example:

ENDBC$ prints stress intensity factors as well as stresses, strains, displacements for entire structure.

ENDBC, SIF$ prints only the stress intensity factors.

APPENDIX B

PROGRAM RESOURCE REQUIREMENT AND AVAILABILITY

Program NOZ-FLAW consists of approximately 17,000 cards in 160 subroutines (FORTRAN IV) and is available in both IBM and CDC versions. When used with the job control language given in this section, the current IBM version requires approximately 1200K bytes of core memory for execution on the Oak Ridge IBM 360/195 computer. Currently, the program is dimensioned for a finite element model not exceeding 500 elements and/or 6000 nodal points. A larger model can be accommodated by modifying four statements in subroutine SETUP to reflect an increase in the maximum number of elements and nodes. In SETUP, the dimension of each array listed below must be greater than or equal to the corresponding expression in parentheses:

IJK (22* [maximum number of elements])
X (maximum number of nodes)
Y (maximum number of nodes)
Z (maximum number of nodes)

Also, the integer values of MAX, NDIM must be set to the following values:

MAX = maximum number of elements
NDIM = maximum number of nodes.

The job control language (JCL) necessary to execute program NOZ-FLAW on the IBM 360/195 computer at Oak Ridge is listed at the end of this section.

Included in the listing is the program overlay structure and the required system I/O disk units. The JCL is organized to link in several double-precision bit manipulation routines written in assembler language. These routines are employed in subroutine FFLDSB to translate the free format input data into the appropriate alphanumeric data for the initialization of variables. Because NOZ-FLAW is written in double precision, the standard single-precision IBM library versions of these routines are not applicable.[1] In mid-FY 81, both the IBM (including assembler language routines) and CDC versions of the NOZ-FLAW source program will be available to the public through the National Energy Software Center at Argonne, Illinois.

---

[1] The CDC source utilizes standard system library routines.

```
//BXBCYLNF JOB (14486),'BR BASS BLK1007'  K25 RM2240 X48718
//*CLASS CPU95=3M,L=75,IO=8,C=0,REGION=1200K
/*
//STEP1 EXEC FORTHCLG,PARM.FORT='MAP,XREF',
//   PARM.LKED='OVLY,MAP,LIST',CLSIZE=498K,
//   PARM.GO='CK=-7,EU=-1,DUMP=I',GOSIZE=1200K,GOTIME=2
//FORT.SYSLIN DD SPACE=(TRK,(300,50),RLSE)
//FORT.SYSIN DD *
=NOZ-FLAW SOURCE PROGRAM
/*
//LKED.ASMHEX DD DSN=A.H.TEA14938.ASMHEX,DISP=SHR,
//  UNIT=3330-1,VOL=SER=CSDCAD
/*
//LKED.SYSIN DD *
 INCLUDE ASMHEX
 INSERT MAIN
 OVERLAY ONE
 INSERT SETUP,MATRED,DIRCOS,MATROT,MESH3D,ELDATA,ADJUST
 OVERLAY ONE
 INSERT
FORMK3,SHAPEB,SHAPEP,SHAPET,SSHAPE,BIGSTF,MFUNC,BNDARY,PRLOAD
 INSERT
BIGPR,SLOPES,VECNIC,CRACK3,ROTATE,CALKMS,STIFF,MATCH,VOLUME
 INSERT AREA,QUDFR,F,F0,INVERT,CALTMP
 OVERLAY ONE
 INSERT
PUZGP3,NDF,PUZSET,PUZSOL,PREFRN,FRONT,FRONTI,TAPS,GAPS,EXPAND
 INSERT
NUM,FRONTS,ZERO,ROWS,SEMBL1,SEMBL2,REDUCE,SETDIS,SETCOR
 INSERT
SCRMBL,SWITCH,FORMNO,BACKSU,BPASS,PRNT0,PRNT1,PRNT2,PRNTA
 INSERT PRNTC,PRNTX
 OVERLAY ONE
 INSERT
POST,INITLP,STPTS,NUMFA,STRSPR,BIGSTR,CROSS,XFORM,PSTRES,K123
 INSERT SUMARY,BOX,FACEP,OUTLIN,ELMP,CONTR,DRAWBL,ROT3D,SIF
 OVERLAY ONE
 INSERT
RZONE3,REZONE,REFINS,FINBC,STRSFG,BSHPF,NORMAL,BSHPL,NMESHF
 INSERT MOVEP,MESH3E
 OVERLAY ONE
 INSERT
AUTO,SETZER,ERROR,CHECK,DEFLT,SETUP2,AMXMN,POINT,CSEGCO,CONST
R
 INSERT
J1LOC,TANGEN,CTHETA,DATAIN,BASE,ELEMNT,AXELMS,DSPLBC,TRCBC
 INSERT NCNSTR,NCNST1,IAVER,JAVER,KAVER,COMGAM
/*
//GO.FT06F001 DD SYSOUT=A
//FT11F001 DD UNIT=SYSDA,SPACE=(TRK,(300,100)),
//  DCB=(RECFM=VBS,BLKSIZE=13030,BUFNO=1,OPTCD=C),
//  DSN=UNIT11,DISP=(,PASS)
//FT12F001 DD UNIT=SYSDA,SPACE=(TRK,(300,100)),
//  DCB=(RECFM=VBS,BLKSIZE=13030,BUFNO=1,OPTCD=C),
```

```
//  DSN=UNIT12,DISP=(,PASS)
//FT13F001 DD UNIT=SYSDA,SPACE=(TRK,(300,100)),
//  DCB=(RECFM=VBS,BLKSIZE=13030,BUFNO=1,OPTCD=C),
//  DSN=UNIT13,DISP=(,PASS)
//FT14F001 DD UNIT=SYSDA,SPACE=(TRK,(300,100)),
//  DCB=(RECFM=VBS,BLKSIZE=13030,BUFNO=1,OPTCD=C),
//  DSN=UNIT14,DISP=(,PASS)
//FT15F001 DD UNIT=SYSDA,SPACE=(TRK,(300,100)),
//  DCB=(RECFM=FB,LRECL=80,BLKSIZE=3200,OPTCD=C),
//  DSN=UNIT15,DISP=(,PASS)
//FT16F001 DD UNIT=SYSDA,SPACE=(TRK,(1500,100)),
//  DCB=(RECFM=VBS,BLKSIZE=13030,BUFNO=1,OPTCD=C),
//  DSN=UNIT16,DISP=(,PASS)
//FT17F001 DD UNIT=SYSDA,SPACE=(TRK,(300,100)),
//  DCB=(RECFM=VBS,BLKSIZE=13030,BUFNO=1,OPTCD=C),
//  DSN=UNIT17
//FT18F001 DD UNIT=SYSDA,SPACE=(TRK,(300,100)),
//  DCB=(RECFM=VBS,BLKSIZE=13030,BUFNO=1,OPTCD=C),
//  DSN=UNIT18,DISP=(,PASS)
//FT19F001 DD UNIT=SYSDA,SPACE=(TRK,(300,100)),
//  DCB=(RECFM=VBS,BLKSIZE=13030,BUFNO=1,OPTCD=C),
//  DSN=UNIT19,DISP=(,PASS)
//FT20F001 DD UNIT=SYSDA,SPACE=(TRK,(300,100)),
//  DCB=(RECFM=VBS,BLKSIZE=13030,BUFNO=1,OPTCD=C),
//  DSN=UNIT20,DISP=(,PASS)
//FT21F001 DD UNIT=SYSDA,SPACE=(TRK,(300,100)),
//  DCB=(RECFM=VBS,BLKSIZE=13030,BUFNO=1,OPTCD=C),
//  DSN=UNIT21,DISP=(,PASS)
//FT22F001 DD UNIT=SYSDA,SPACE=(TRK,(300,100)),
//  DCB=(RECFM=VBS,BLKSIZE=13030,BUFNO=1,OPTCD=C),
//  DSN=UNIT22,DISP=(,PASS)
//FT23F001 DD UNIT=SYSDA,SPACE=(TRK,(300,100)),
//  DCB=(RECFM=VBS,BLKSIZE=13030,BUFNO=1,OPTCD=C),
//  DSN=UNIT23,DISP=(,PASS)
//FT05F001 DD *
=INPUT DATA DECK
/*
//
ENDINPUT
```

APPENDIX C

SAMPLE INPUT AND OUTPUT

Input data that were provided for the three different NOZ-FLAW analyses of an ITV model reported in Chapter 3 (see Figures 13, 16) are given below. A quarter-circular flaw (MATH, a/b = 0.41, a = 9.5 cm) was analyzed under internal pressure loading (100 MPa) both with and without crackface pressure (100 MPa). A similar experimentally measured flaw (EXPR) from Reference 18 was also analyzed under internal pressure loading (100 MPa) with applied crackface pressure (100 MPa).

A complete printout for the quarter-circular flaw model with applied crackface pressure is provided on microfiche and attached to the back cover. NOZ-FLAW prints an echo of the input data, nodal global coordinates and element connectives, imposed boundary conditions, stresses, strains, and displacements throughout the structure, and the mode I, II, and III stress intensity factors for each of the special crack tip elements along the flaw front.

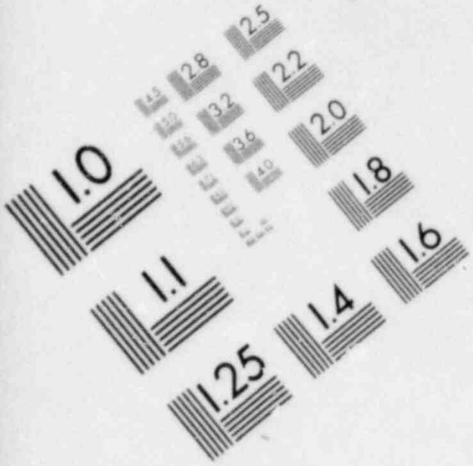

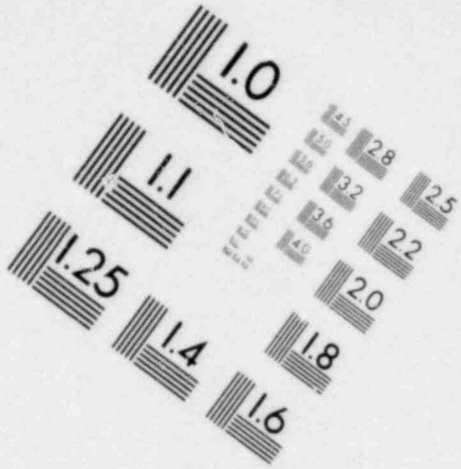

IMAGE EVALUATION TEST TARGET (MT-3)

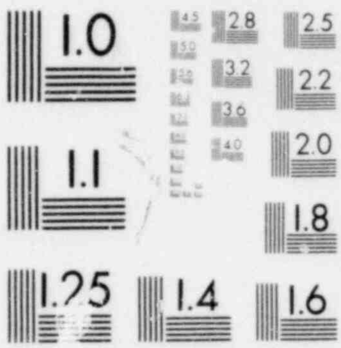

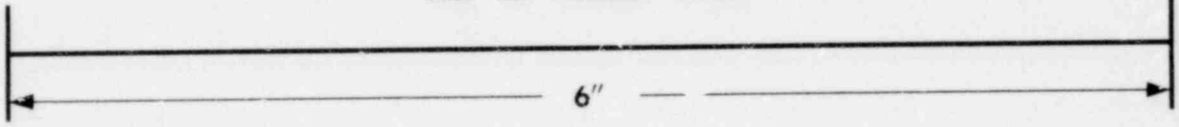

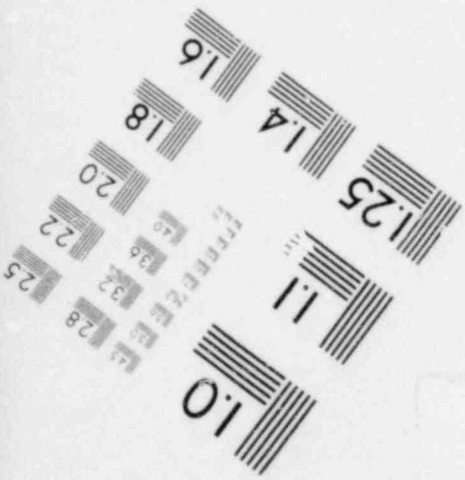

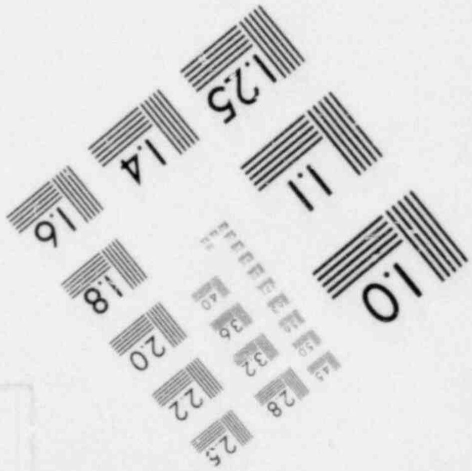

IMAGE EVALUATION
TEST TARGET (MT-3)

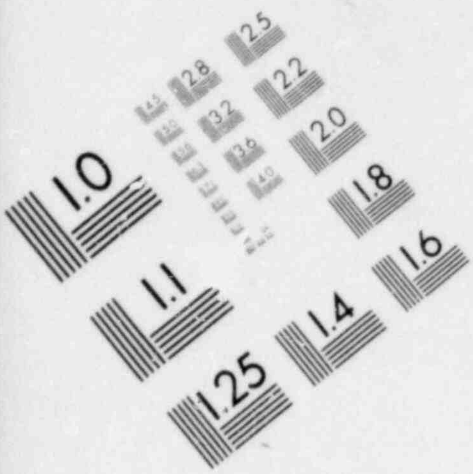

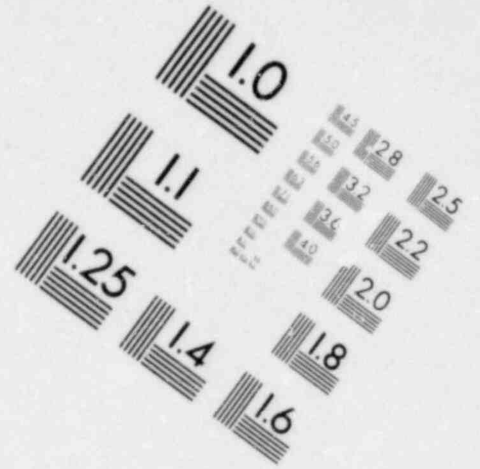

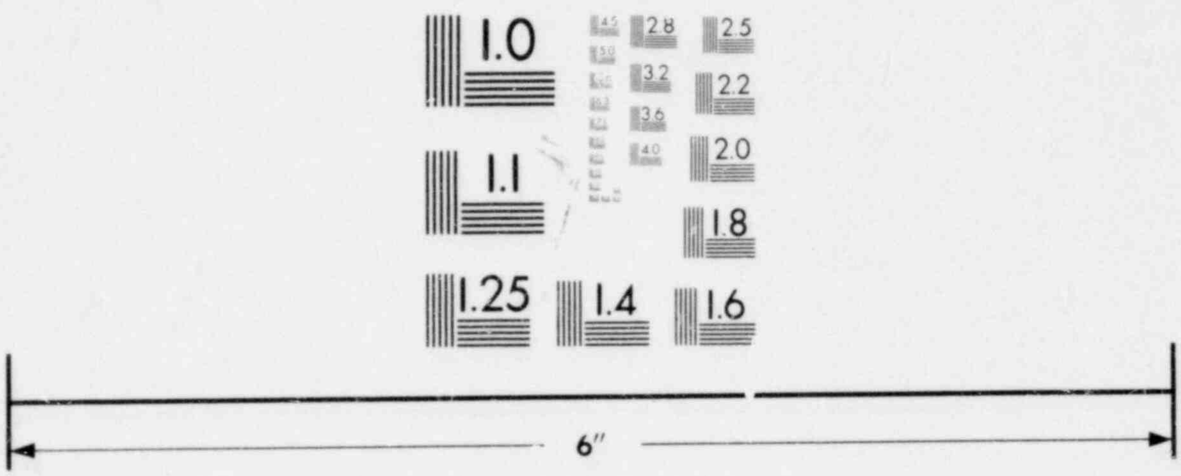

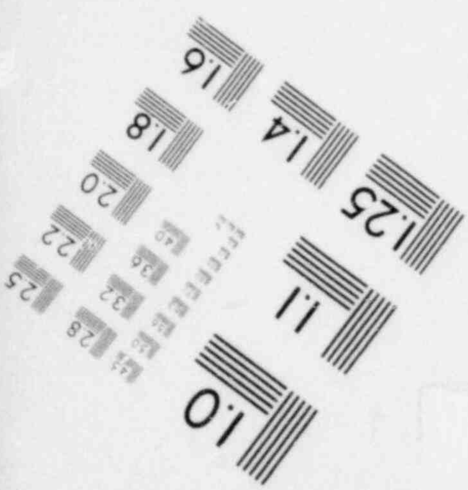

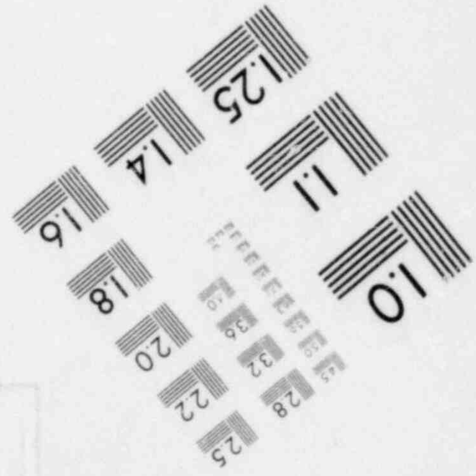

Input data for ITV model with a quarter-circular flaw (MATH) under internal pressure loading and crackface pressure.

```
AUTO
$ITV NOZZLE CORNER FLAW
NOZZLE, 3.E7, .3, NDCORNER, .125$
MATH, .343,.152,.114,.102,1.,1.,.038,.076,.670,.721,.152,6$
2,2,2,1,2,1,4,0.005,1.5$
0.11,0.11$
CRPRESS, 100.$
CYPRESS, 100.$
ENDCAP, 100.$
ENDBC$
```

Input data for ITV model with a quarter-circular flaw (MATH) under internal pressure loading without crackface pressure.

```
AUTO
$ITV NOZZLE CORNER FLAW
NOZZLE, 3.E7, .3, NDCORNER, .125$
MATH,.343,.152,.114,.102,1.,1.,.038,.076,.670,.721,.152,6$
2,2,2,1,2,1,4,0.005,1.5$
0.11,0.11$
CYPRESS,100.$
ENDCAP,100.$
ENDBC$
```

Input data for ITV model with an experimentally measured flaw (EXPR) under internal pressure loading and crackface pressure.

```
AUTO
$ITV NOZZLE CORNER FLAW
NOZZLE, 3.E7,.3,NDCORNER,.125$
EXPR,.343,.152,.114,.102,1.,1.,.038,.076,.670,.721,.152,6$
2,2,2,1,2,1,4,0.0,1.5$
.118,.119,.108,.076,.045,.012,0.,0.,.012,.045,.076,.108,.117,.118$
CRPRESS,100.$
CYPRESS,100.$
ENDCAP,100.$
ENDBC$
```

NUREG/CR-1843
ORNL/NUREG/CSD/TM-18
Dist. Category RF

INTERNAL DISTRIBUTION

1-5. B. R. Bass
6-8. R. H. Bryan
9-13. J. W. Bryson
14. D. A. Canonico
15. H. P. Carter/A. A. Brooks/ CSD Library
16. R. D. Cheverton
17. J M. Corum
18. W. R. Corwin
19. G. J. Farris
20. W. L. Greenstreet
21. R. C. Gwaltney
22. P. P. Holz
23. S. K. Iskander
24. J. G. Merkle
25. S. E. Moore
26. F. R. Mynatt
27-31. R. E. Textor
32. H. E. Trammell
33-34. G. D. Whitman
35. Patent Office
36. Central Research Library
37. Document Reference Section - Y-12
38. Engineering Physics Information Center
39-41. Laboratory Records Department
42. Laboratory Records (RC)
43. ORGDP CSD Library
44. ORGDP Library
45. ORGDP Plant Records

EXTERNAL DISTRIBUTION

46. C. Z. Serpan, Reactor Safety Research, Nuclear Regulatory Commission, Washington, DC 20555
47. M. Vagins, Reactor Safety Research, Nuclear Regulatory Commission, Washington, DC 20555
48. Office of Assistant Manager for Energy Research and Development, DOE, ORO, Oak Ridge, TN 37830
49-50. Technical Information Center, DOE, Oak Ridge, TN 37830
51-480. Given distribution as shown in category RF (10 copies - NTIS)

☆U.S. GOVERNMENT PRINTING OFFICE: 1980-740-062/497